

MUSE Simulation

Steffen Strauch
University of South Carolina

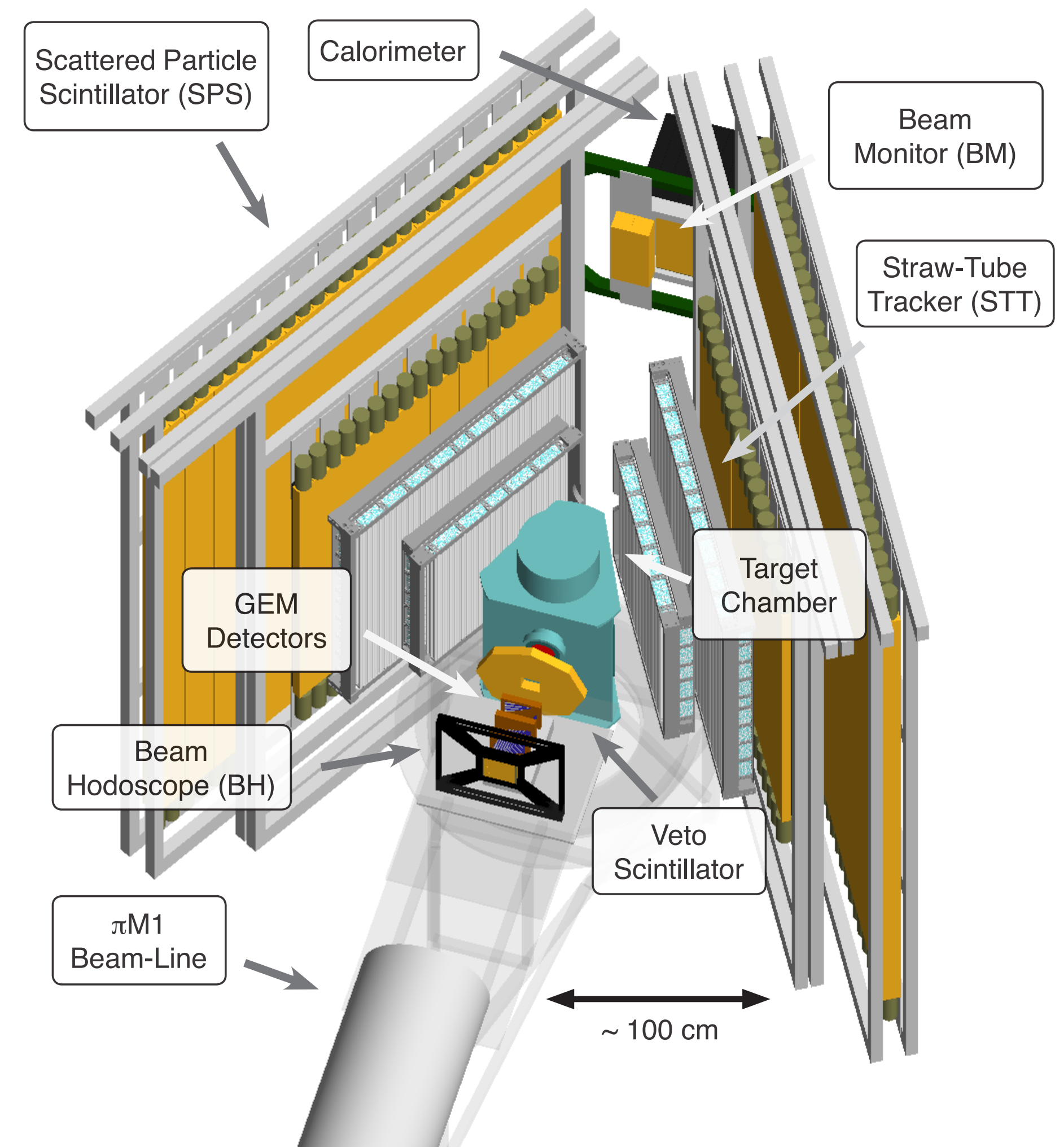
for the MUSE Collaboration

Supported in parts by the U.S. National Science Foundation: NSF PHY-2111050 (USC).
The MUSE experiment is supported by the U.S. Department of Energy, the U.S. National Science Foundation, the Paul Scherrer Institute,
and the US-Israel Binational Science Foundation.

MUSE Review, BVR 54, PSI, January 23, 2023

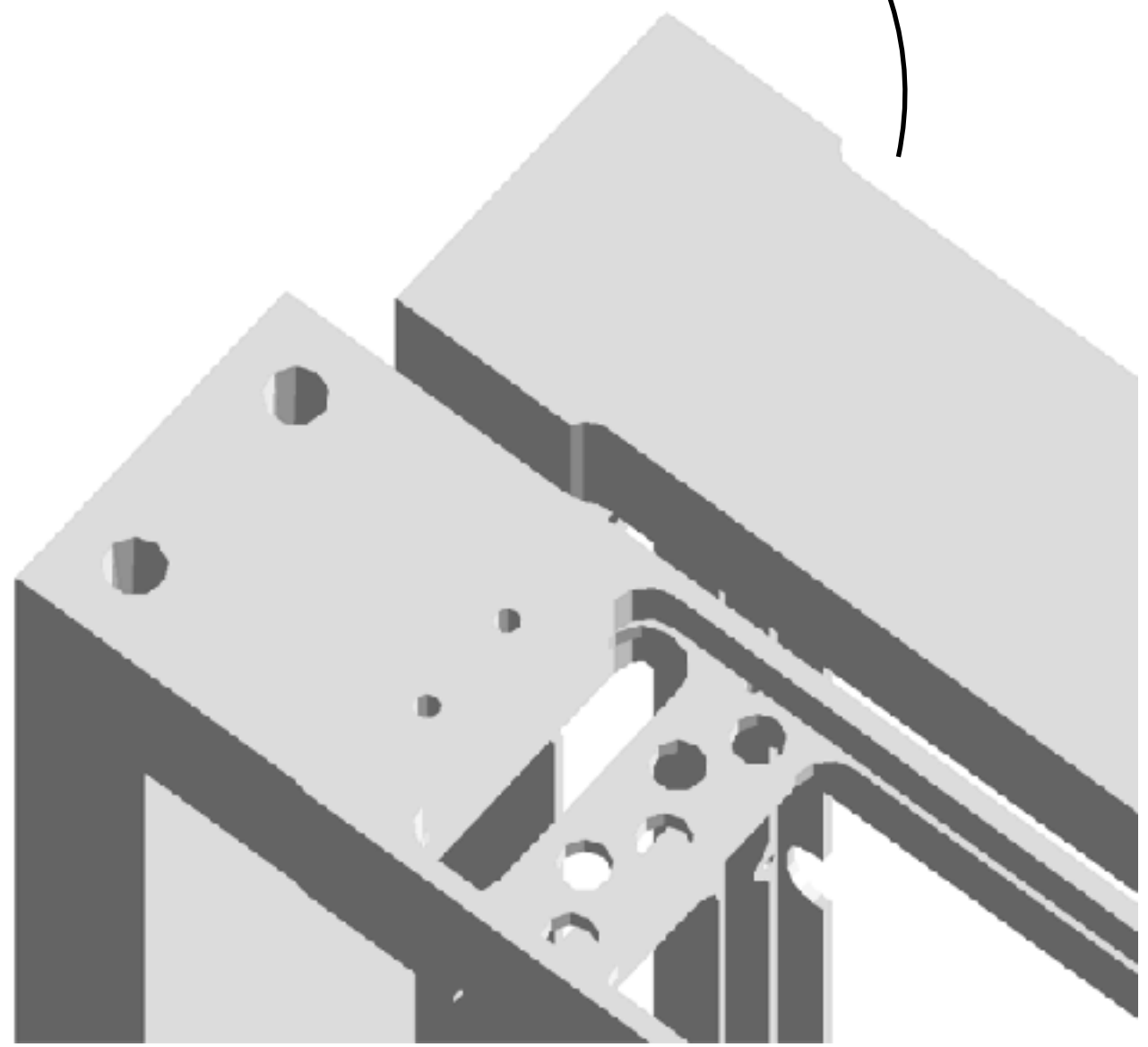
Recent updates of the MUSE simulation

- More detailed and accurate geometry
- Flexible alignment of components
- More realistic particle beam
- Digitization of simulated events
- Realistic event generator to study radiative effects, $ep \rightarrow e\gamma$ [BVR 52]



Implementation of the STT frames in the MUSE simulation

Simplified CAD model (Tom O'Connor, ANL) with detail in outer surface maintained



Binary STL files can now be loaded directly in the simulation.

More work needed to bring all relevant structure material into the simulation.

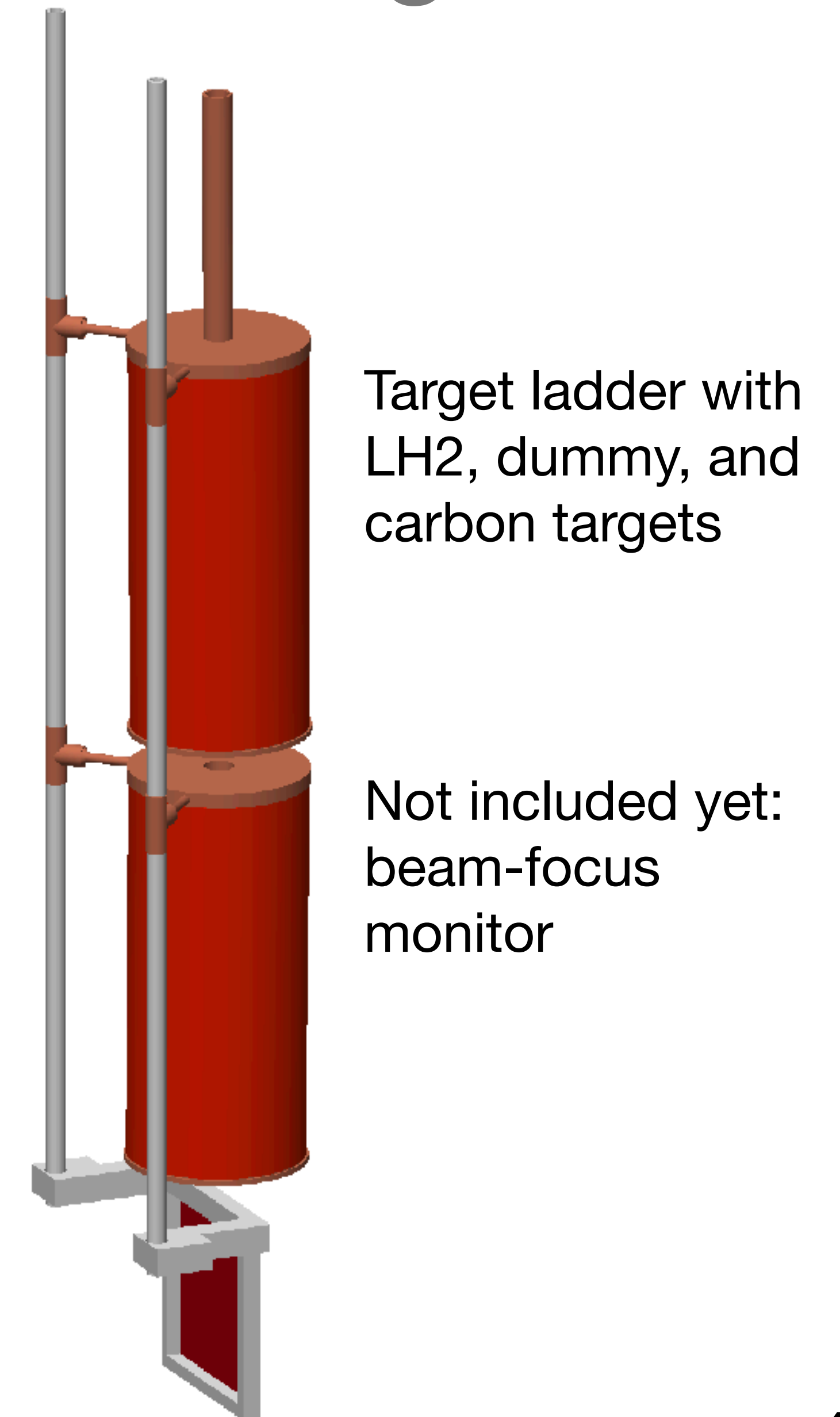
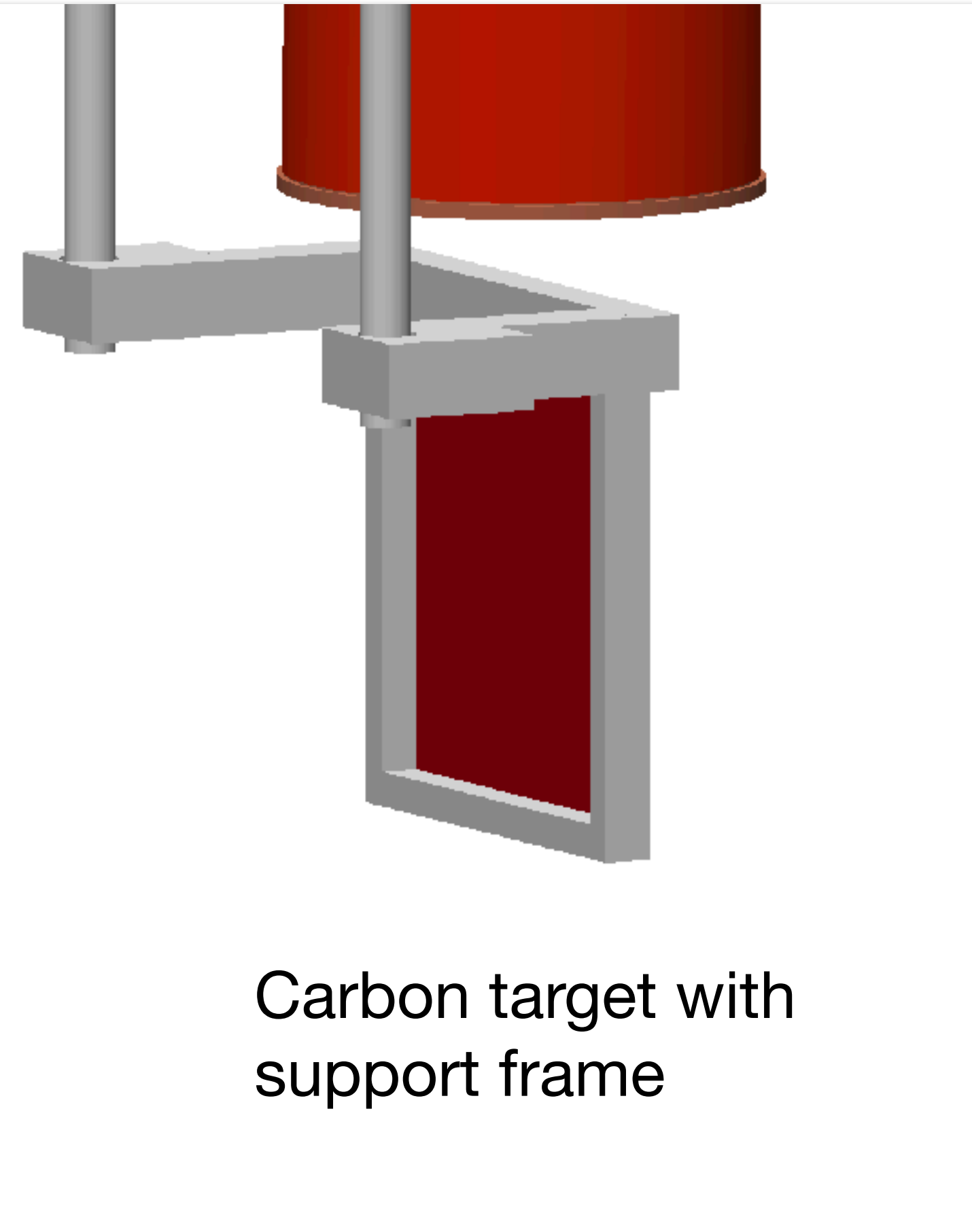
Full CAD model

Technical drawing of a full CAD model of a mechanical assembly. The drawing includes a main view of the assembly, a detail view labeled 'DETAIL A SCALE 1:1', and a parts list table. The parts list table is as follows:

ITEM NO.	PART NUMBER	Material	Default
1	Stack Small Y.REV01		2
2	C-03-00 Inner frame B1	See BOM	1
3	DIN EN ISO 1207 - M2.5 x 5 - 8N		44
4	DIN 912 M4 x 12 - 12C	Material <not specified>	16

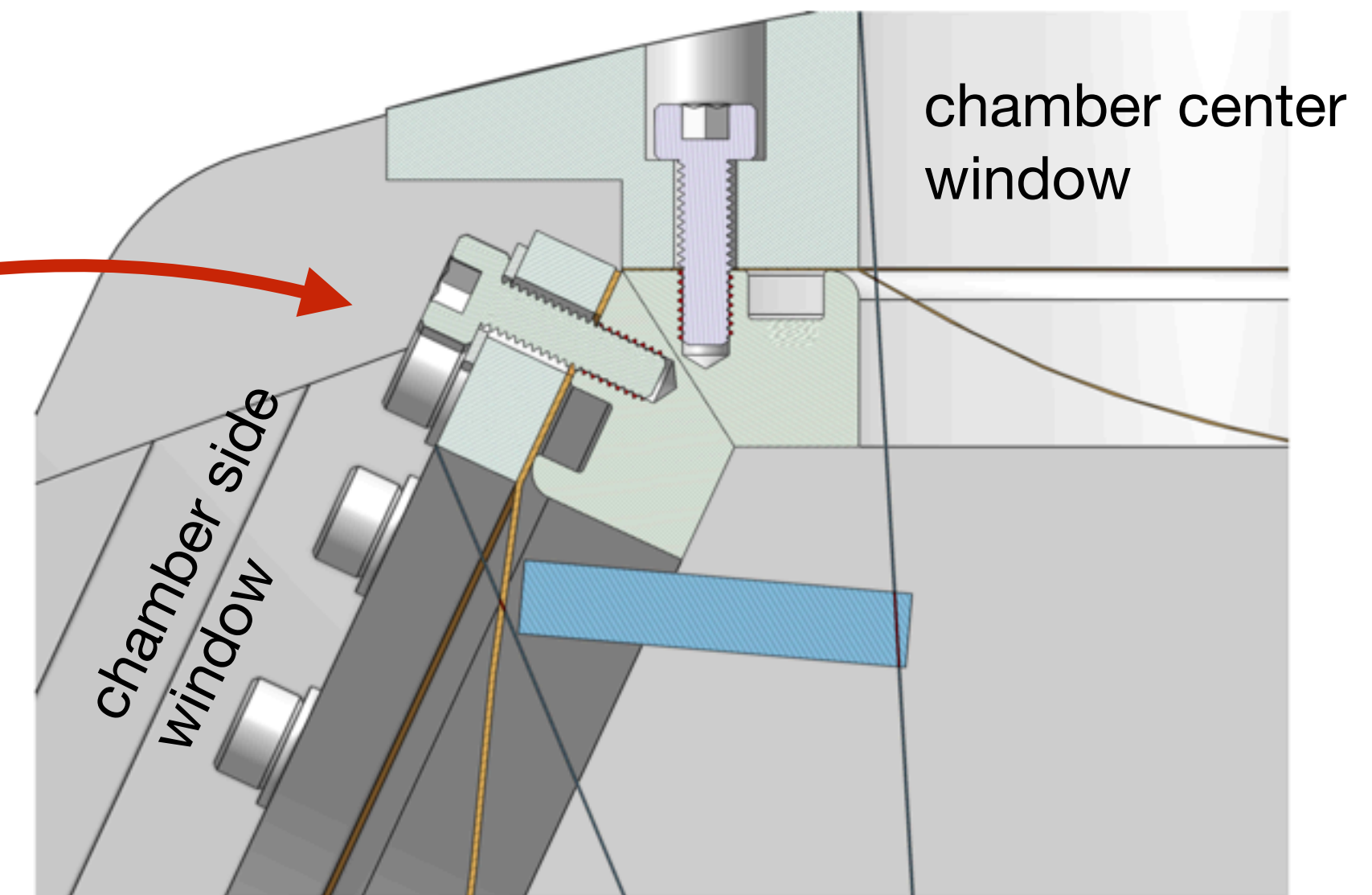
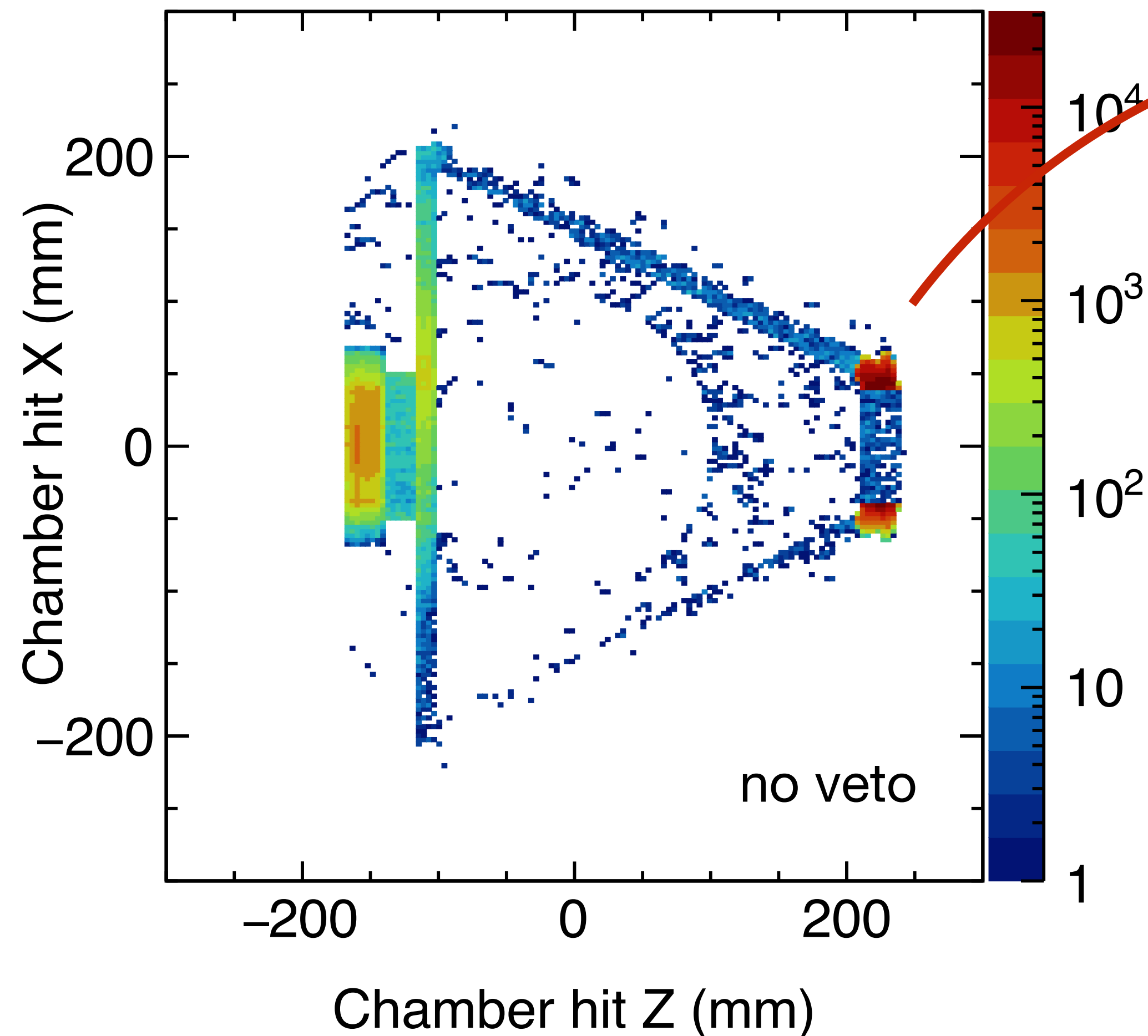
Additional information from the drawing includes a revision table at the top right and a detailed parts list at the bottom right.

Reimplementation of target ladder including carbon target



Scattering off the target chamber contributes significantly to the total DAQ rate

Simulated scattering-chamber hits by a 161 MeV/c electron beam with trigger on the beam-left ($x > 0$)
SPS detectors, no target

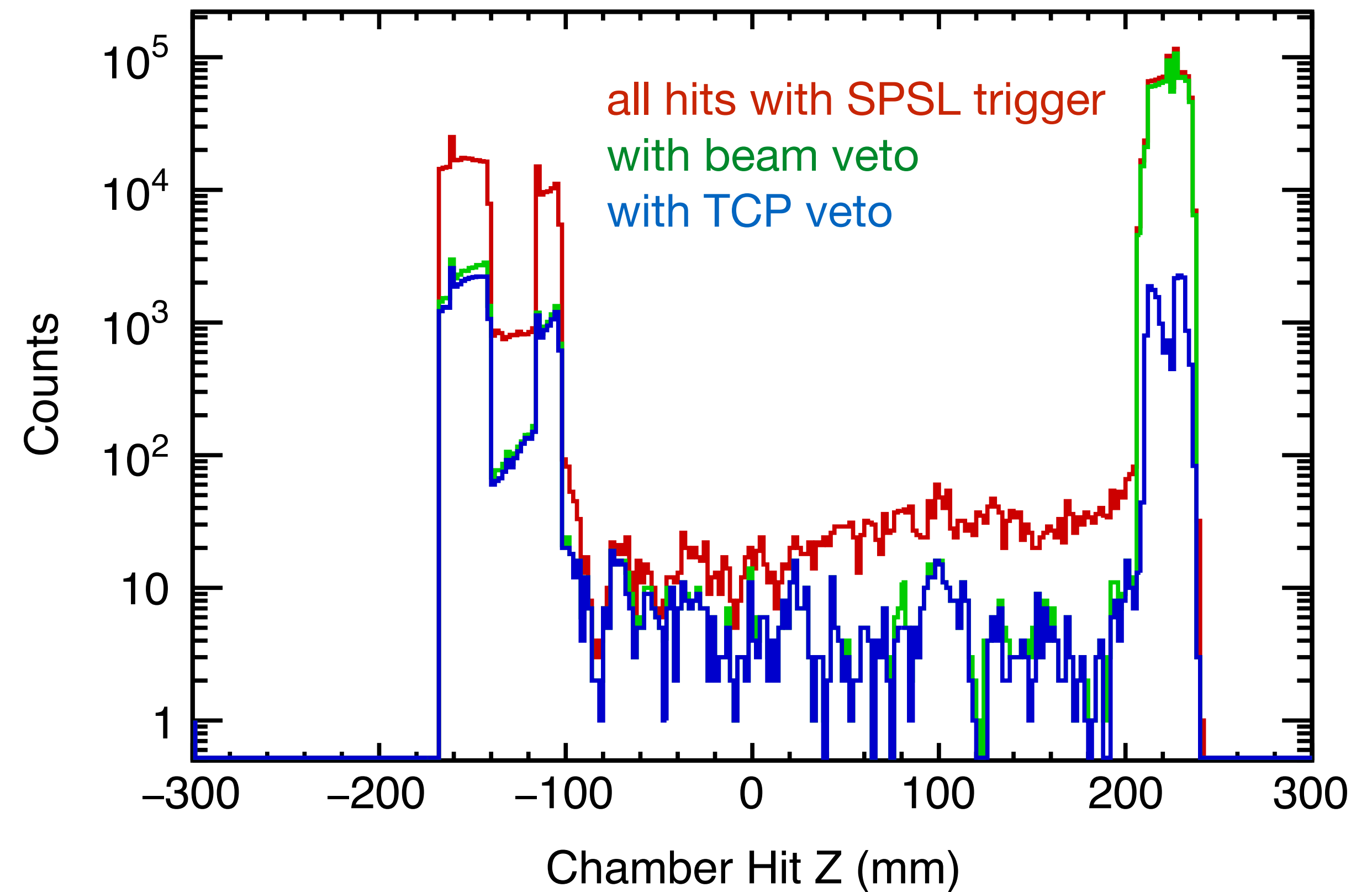
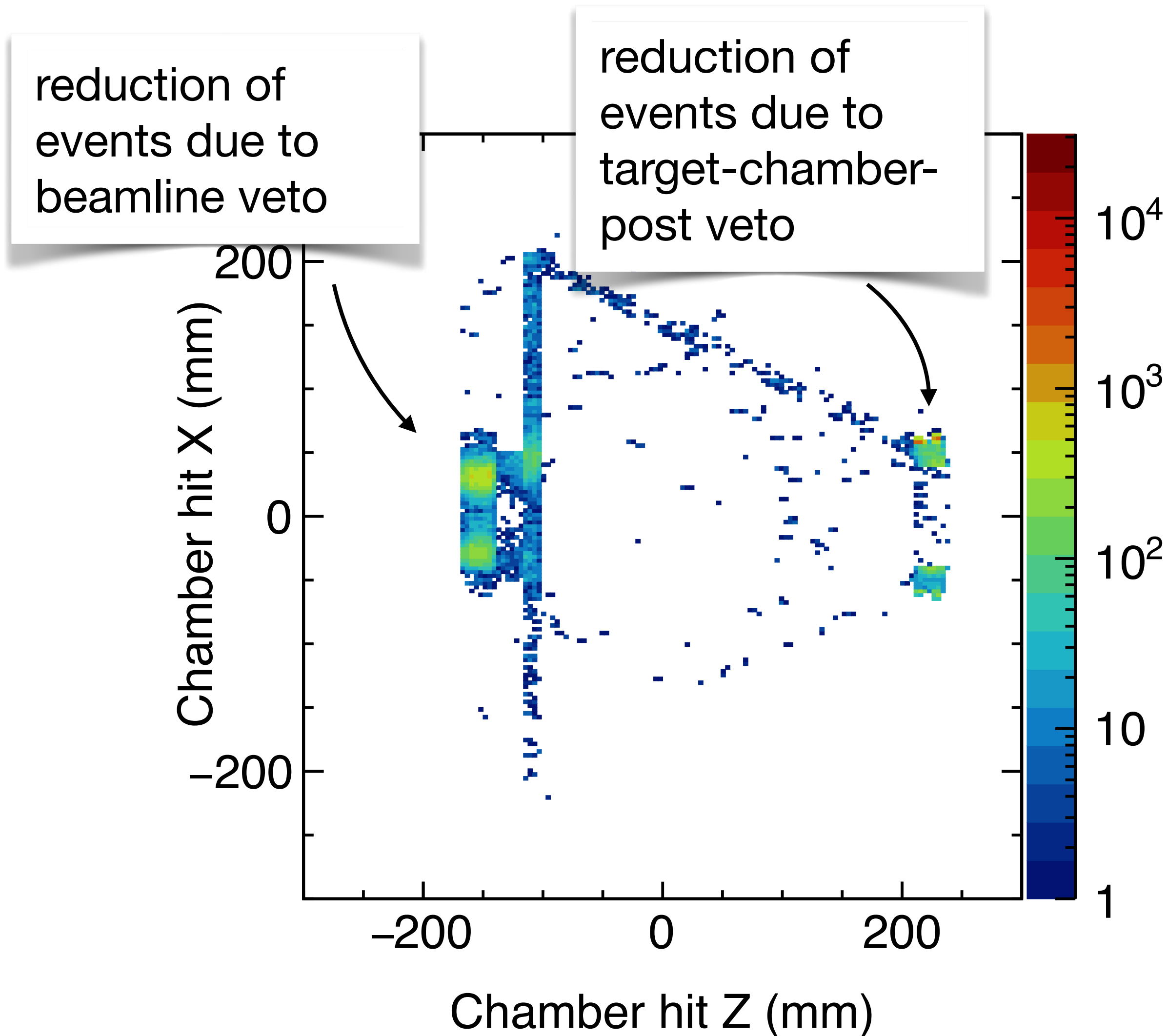


Target chamber post veto detector:

(T. Rostomyan)

- Must be inside of the chamber.
- Maximum coverage of chamber posts, while clearing the acceptance of scattering and straight through events, and
- clearing in-bound **chamber side window**

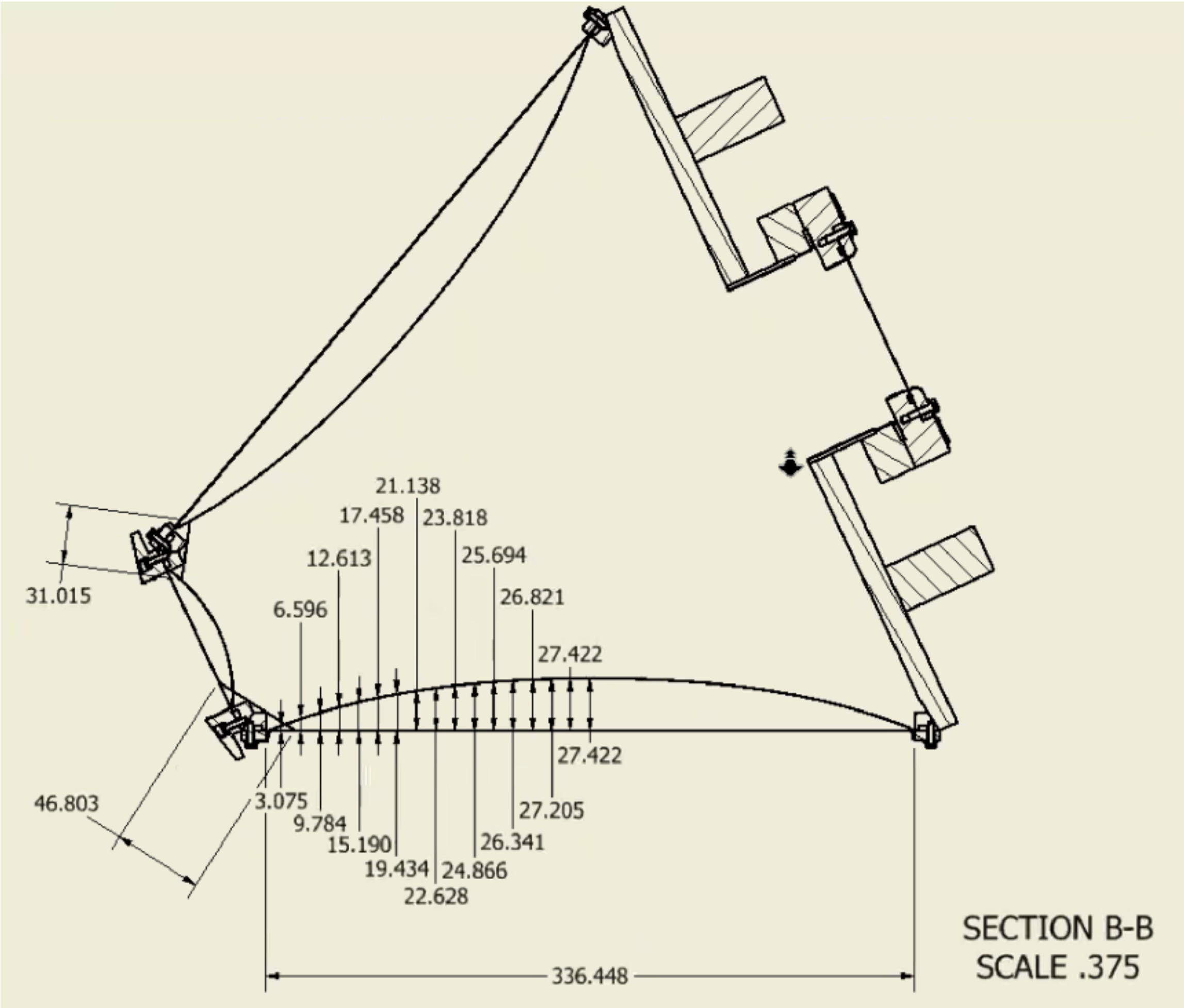
Anticipated suppression of chamber hits: Fewer than 10% remaining



Planned simulation geometry update

The chamber windows bow inwards when the chamber is under vacuum

A more realistic shape of the side-exit window is needed in the simulation to properly simulate the correct **material thickness for all scattering angles.**



Drawing by Tom O'Connor (ANL)

Detector positions in the simulation define the geometry used in the data analysis

- Implement the geometry consistent with design or known as-built geometry



- **Survey the setup**
- Modify geometry of simulation to **fit survey data**



- Export geometry as GDML file for use in data analysis

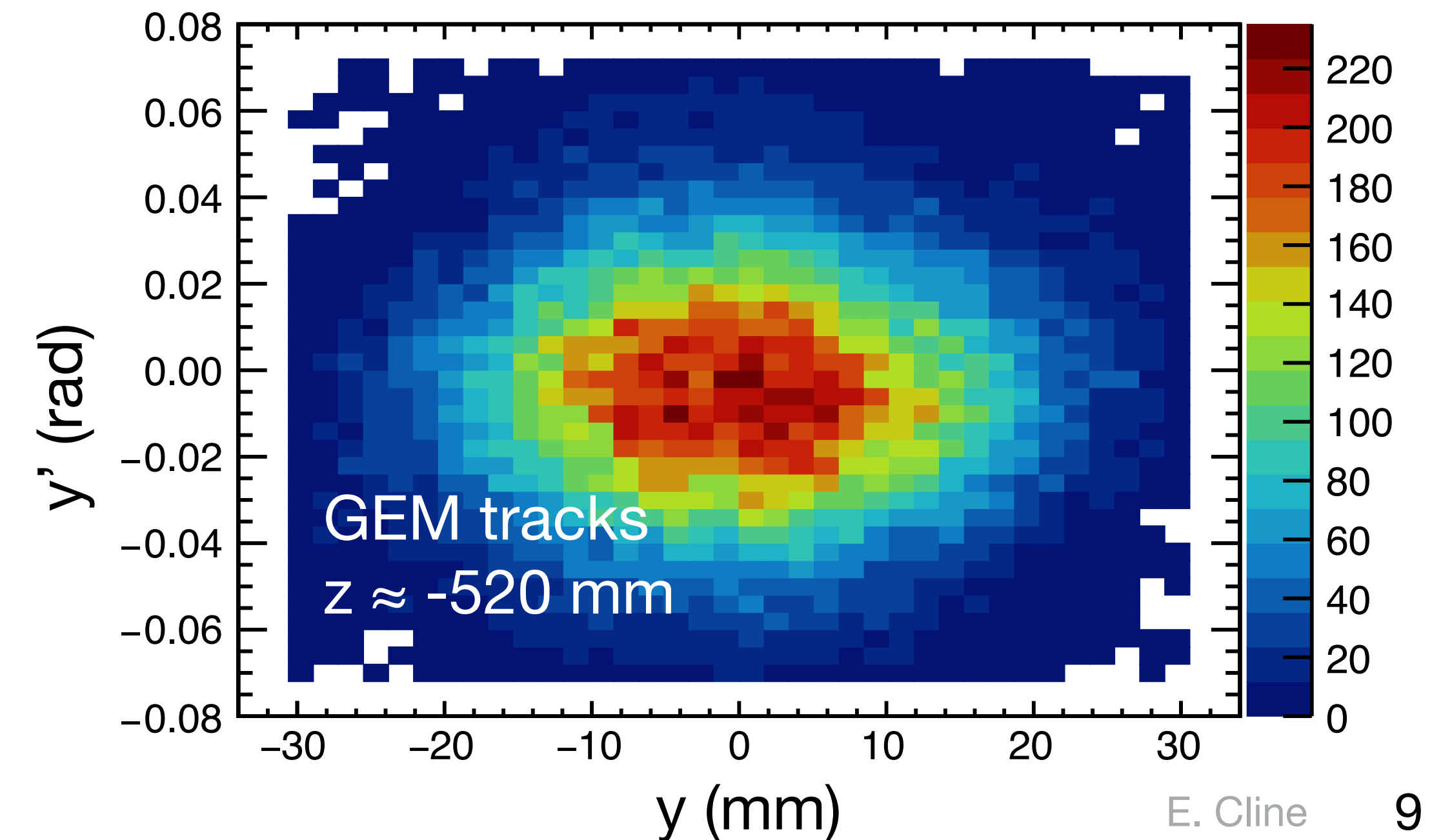
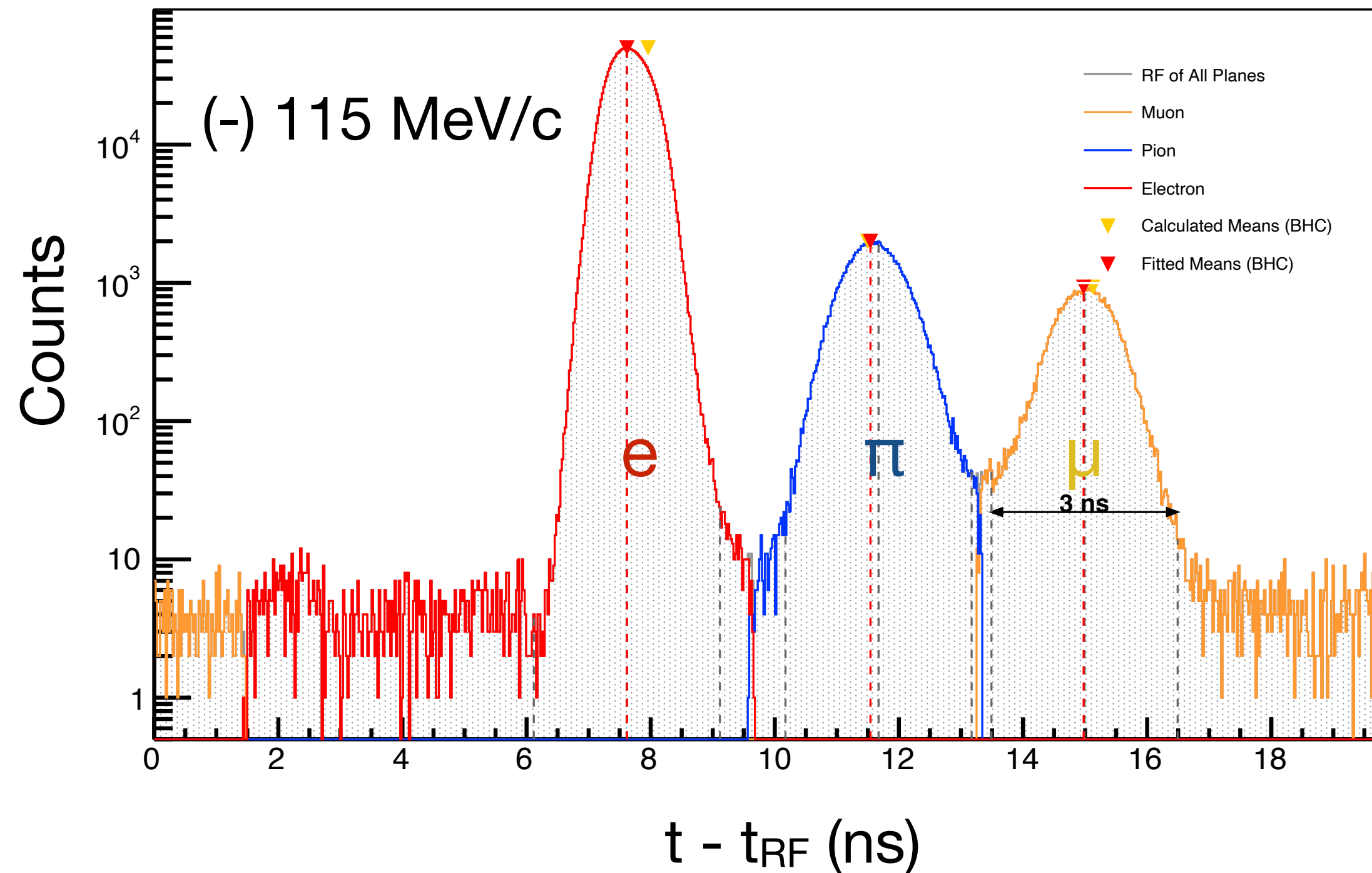
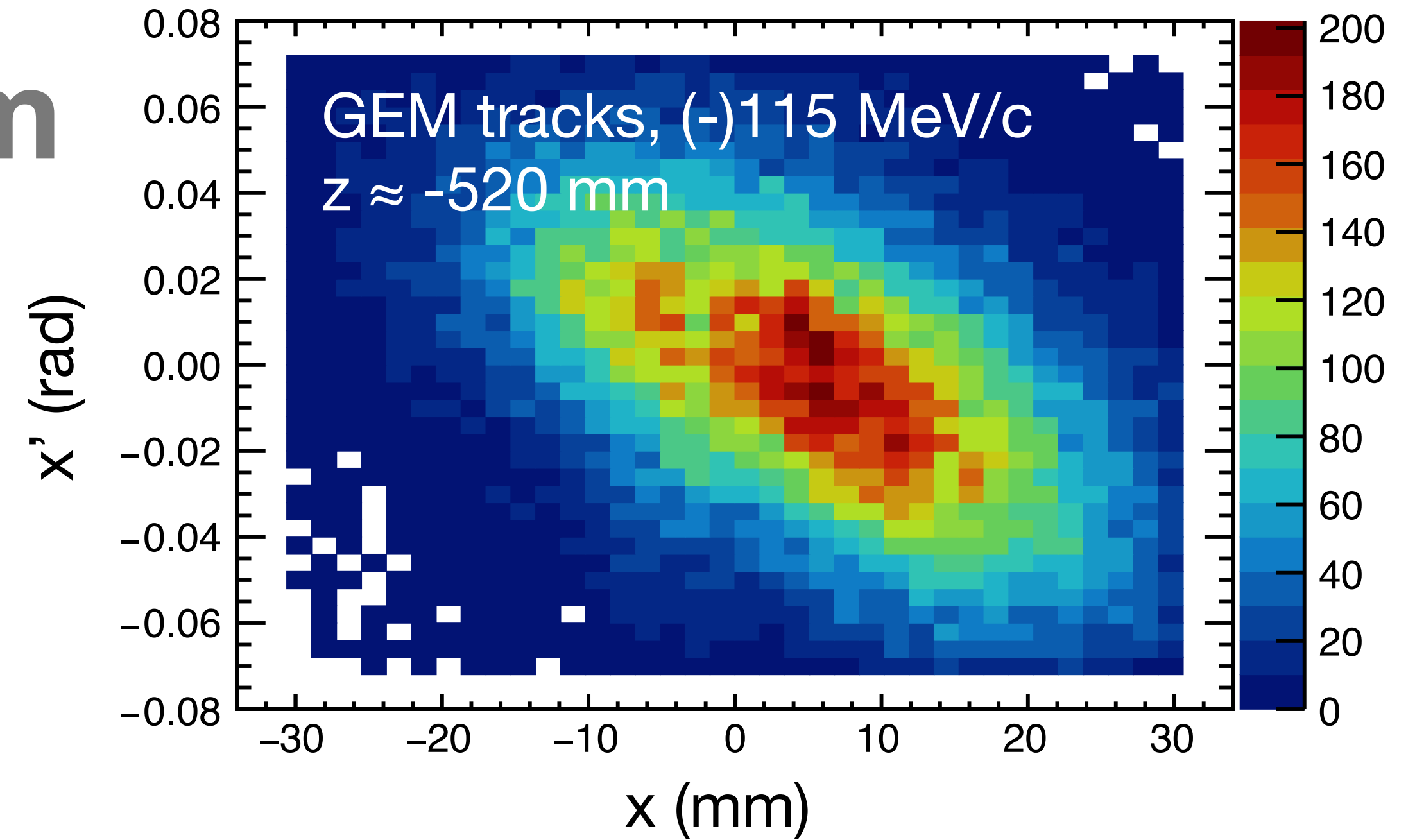
Example fit result

/g4PSI/det/trans	GEM0	-0.511	0.106	-0.008 mm
/g4PSI/det/trans	GEM1	-1.034	1.020	-4.803 mm
/g4PSI/det/trans	GEM2	-0.754	0.246	0.937 mm
/g4PSI/det/trans	GEM3	-1.151	0.304	0.065 mm
/g4PSI/det/rot	GEM0	0.036	0.018	-0.541 deg
/g4PSI/det/rot	GEM1	-0.666	-0.233	-6.706 deg
/g4PSI/det/rot	GEM2	-0.075	1.132	-1.290 deg
/g4PSI/det/rot	GEM3	0.032	-0.164	-0.223 deg

fit translational and rotational offsets

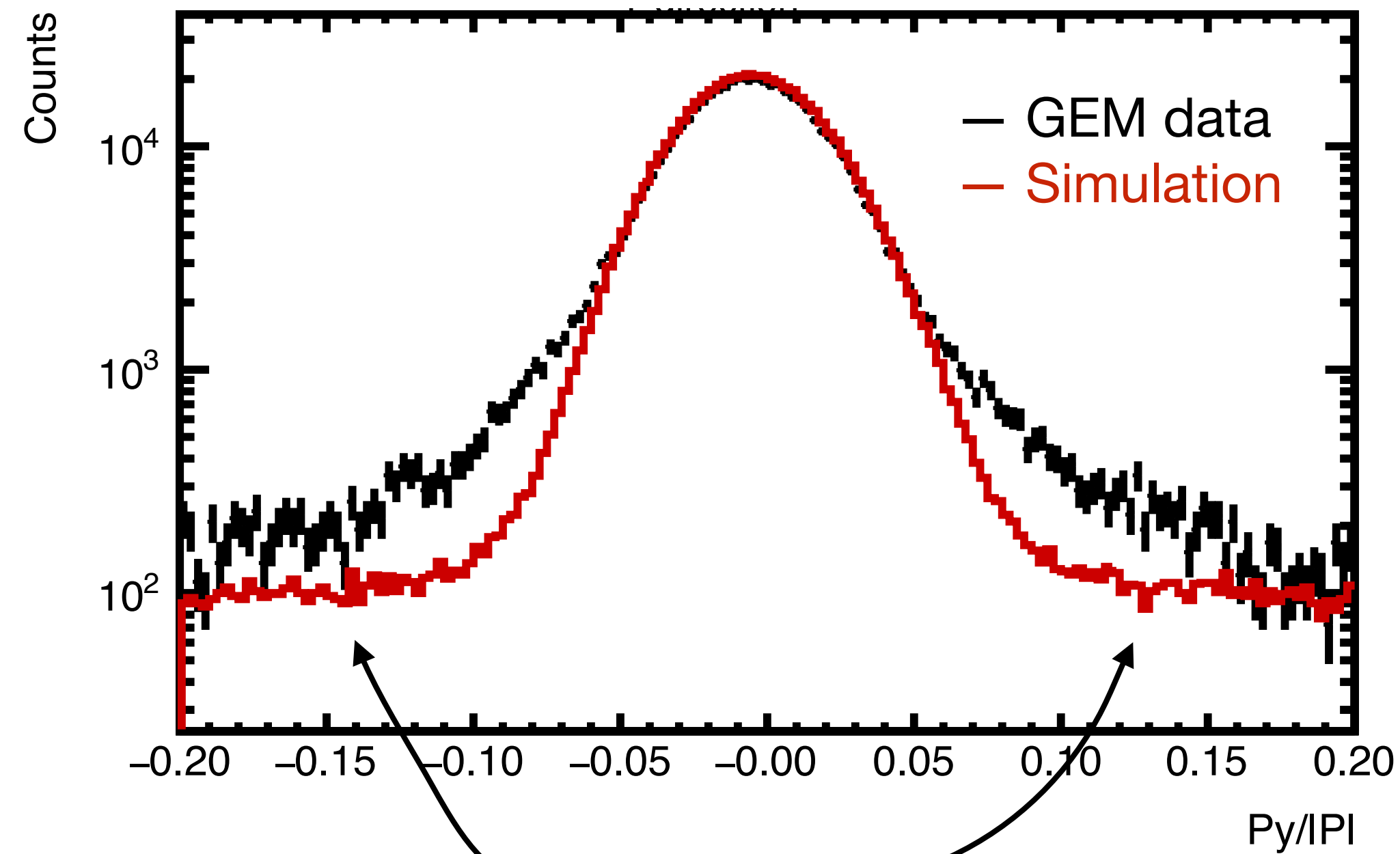
Modeling the particle beam

- Particle mix
- Position and direction distributions including (new) correlations



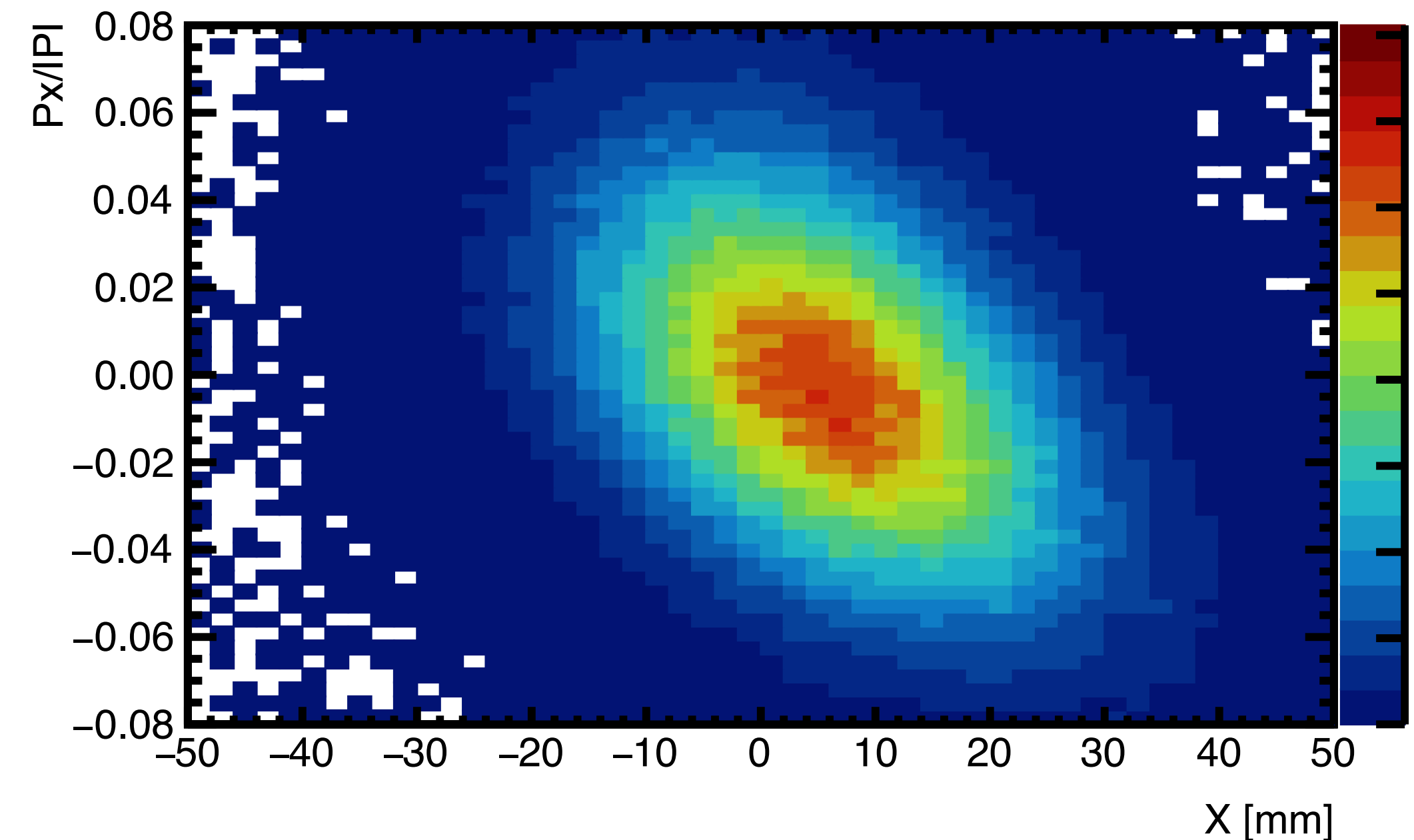
g4PSI Beam parameter tune to GEM-track distribution

Beam direction in y
(Simulation and data)



Tails from secondary particles

Correlation of beam direction and
position along x (Simulation)



M. Nicol

Presently, all beam particle types in the simulation are assumed to have the same distributions.

All simulated detector responses are now digitized for analysis

Detectors	g4PSI	Digitization
SPS, BM, BH, VETO	g4PSIScintillatorSD	✓
CAL	g4PSICherenkovSD	✓
STT	g4PSITrackerSD	✓
GEM	g4PSITrackerSD	✓

Digitization of a simulated energy deposition of E at position x in a scintillator

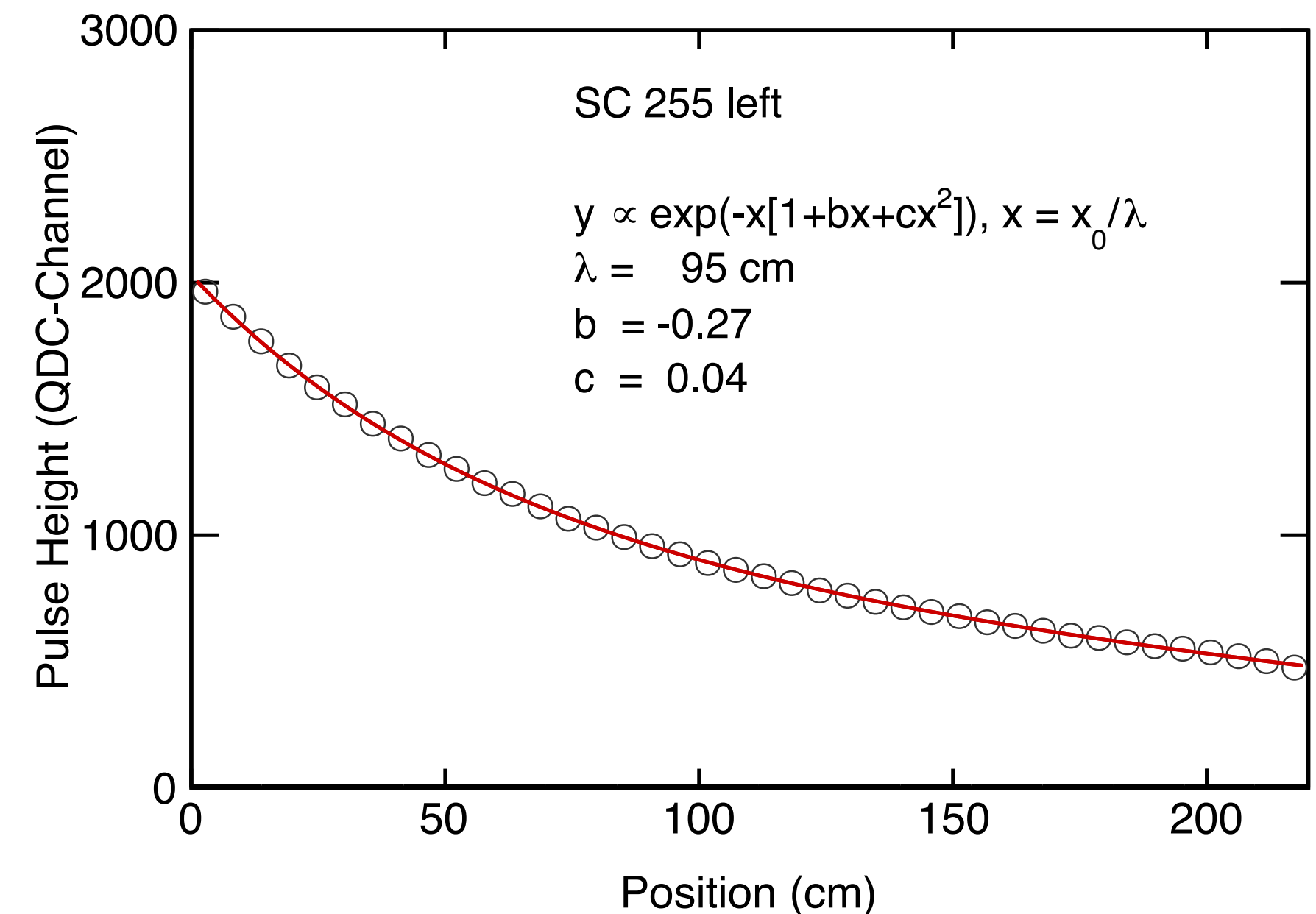
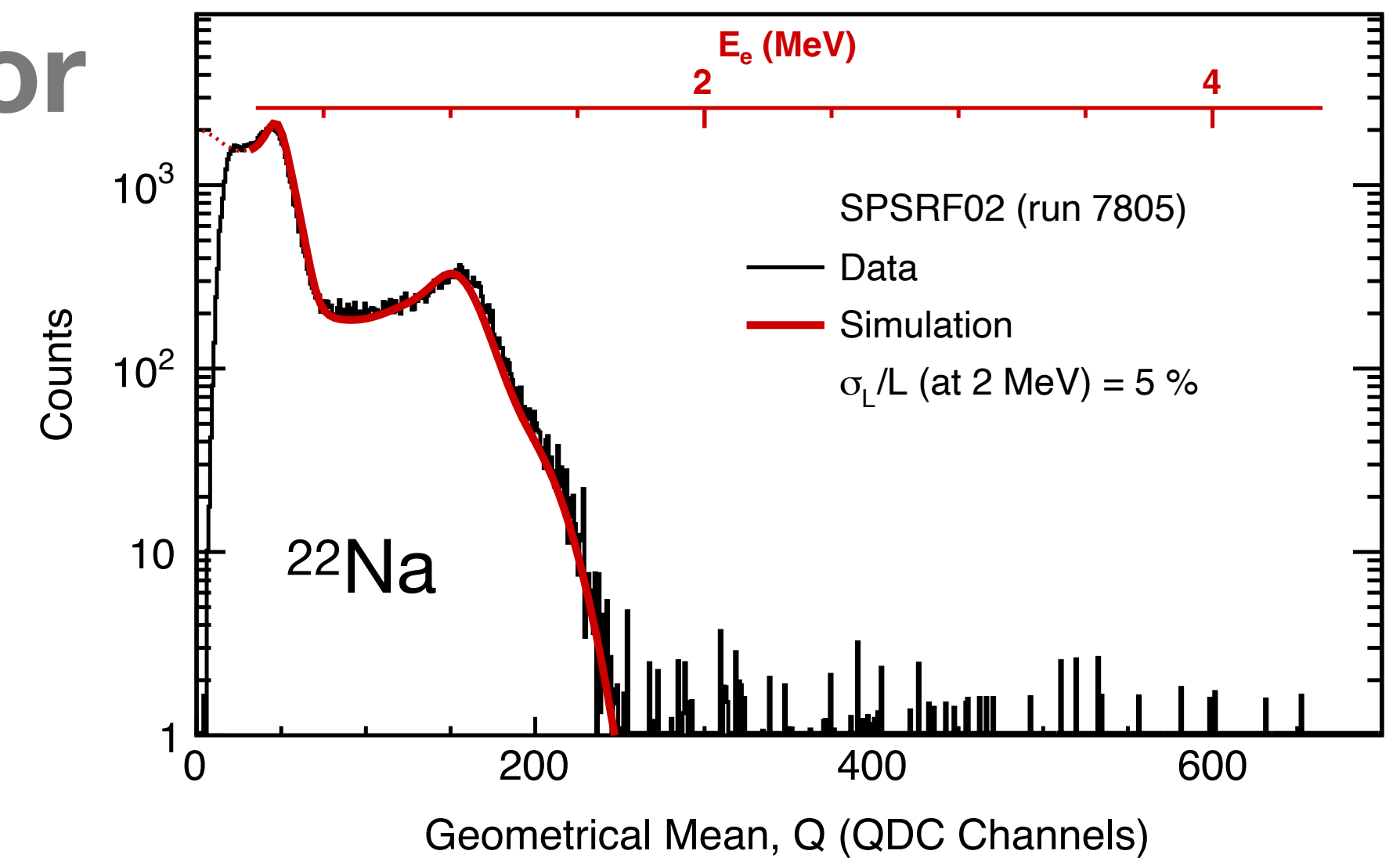
Digitized light output at the two PMTs:

$$Q_1(E, x) = g_1 EA_1(x)$$

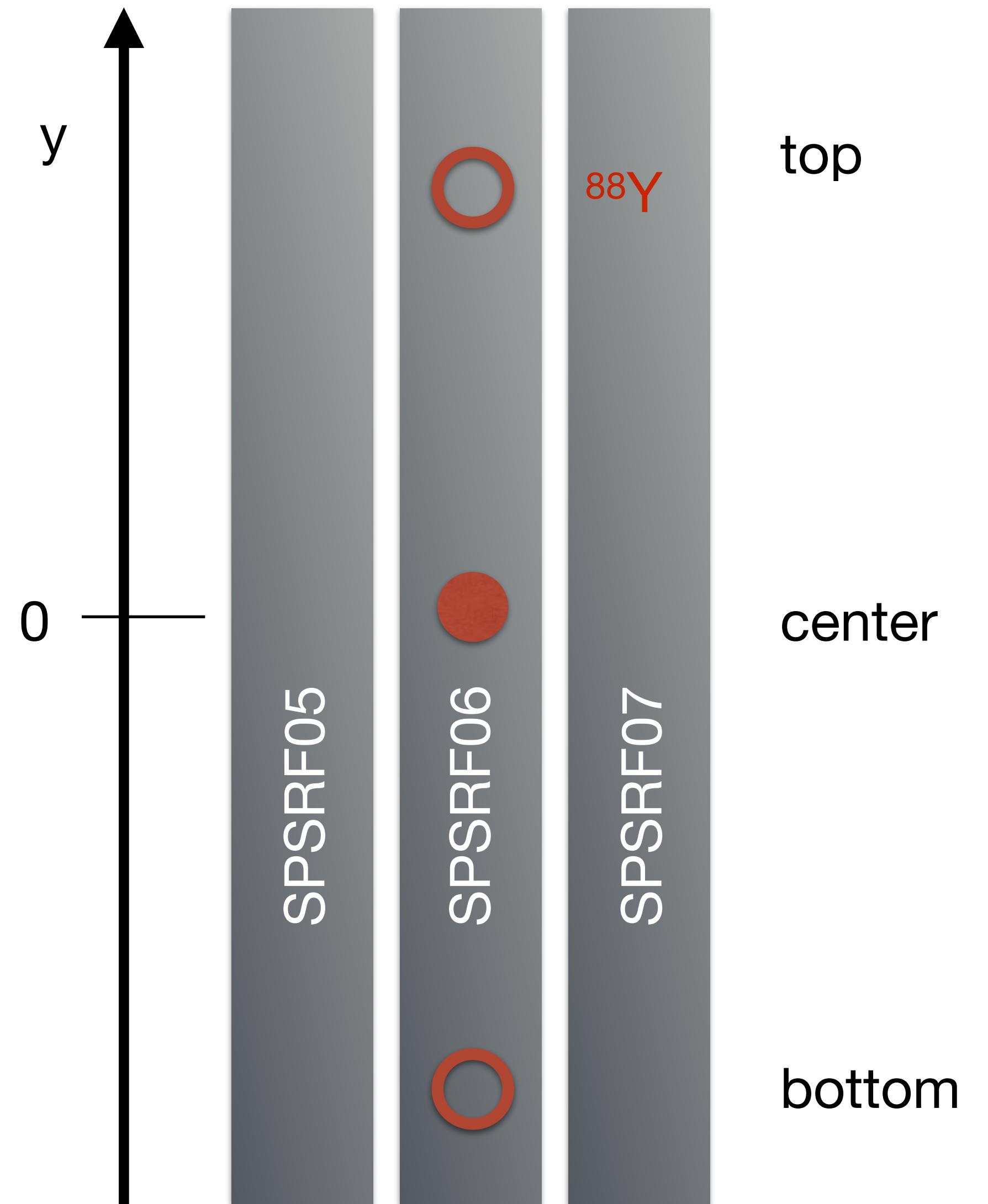
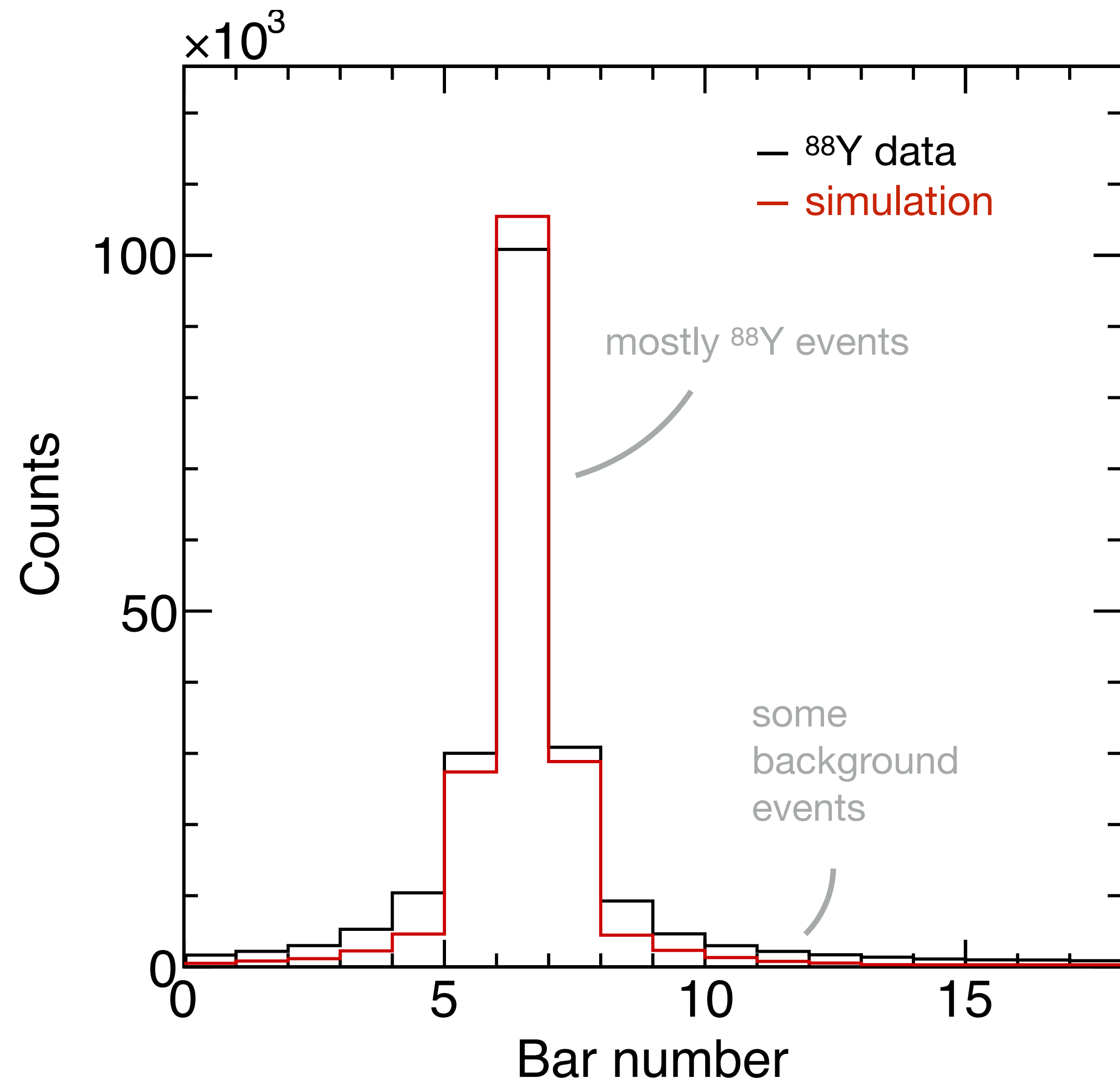
$$Q_2(E, x) = g_2 EA_2(L - x)$$

Detector characteristics that enter the digitization

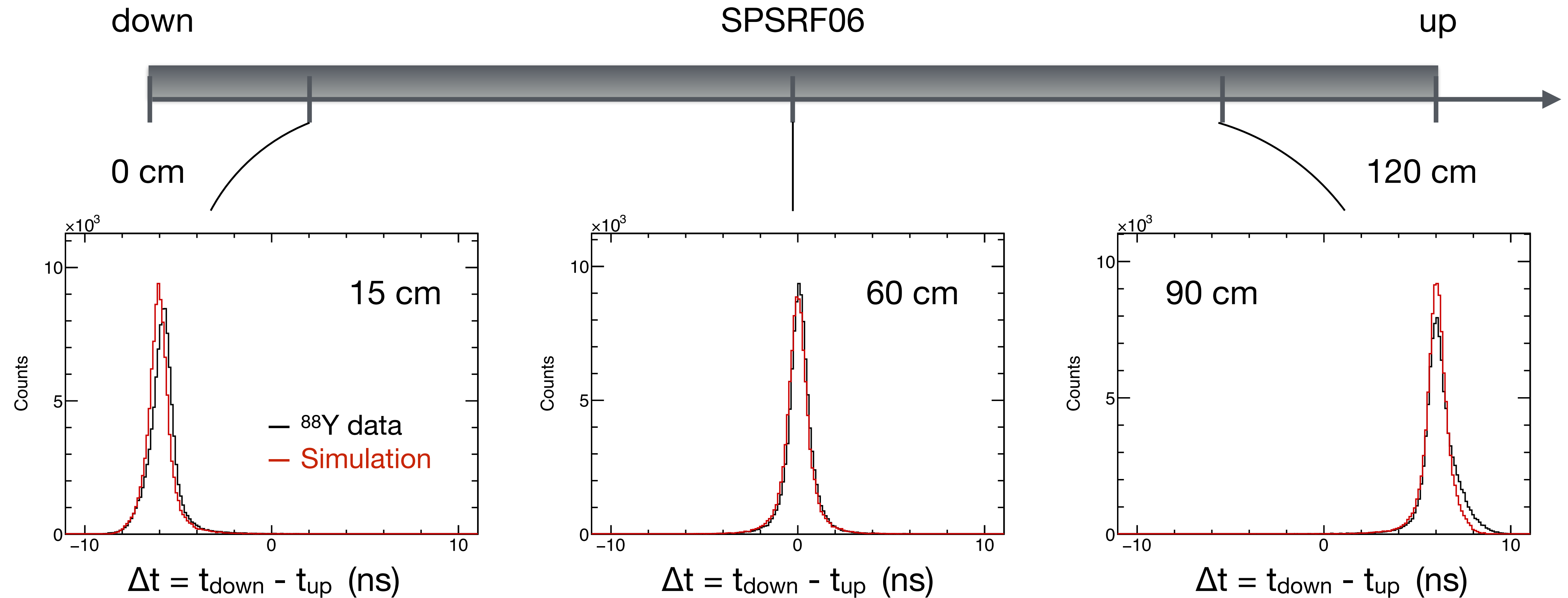
- Pedestals
- Gains and light-output resolution
- Attenuation function, $A(L/2) = 1$
- Effective speed of light
- Time-walk correction
- Time resolution
- Discriminator threshold



^{88}Y calibration to test detector response and simulation close to threshold



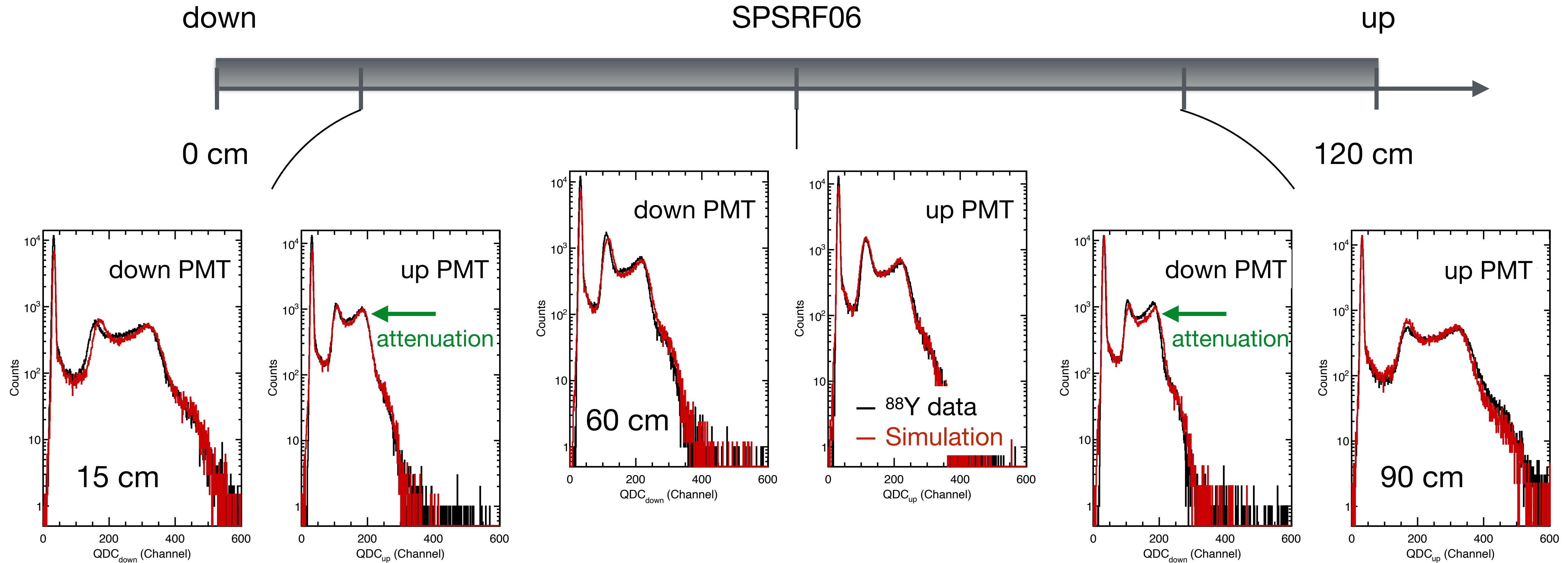
Simulated time response, $\Delta t = t_{\text{down}} - t_{\text{up}}$



$$\Delta t = t_{\text{down}} - t_{\text{up}} = \frac{1}{c_{\text{eff}}} (2x - L)$$

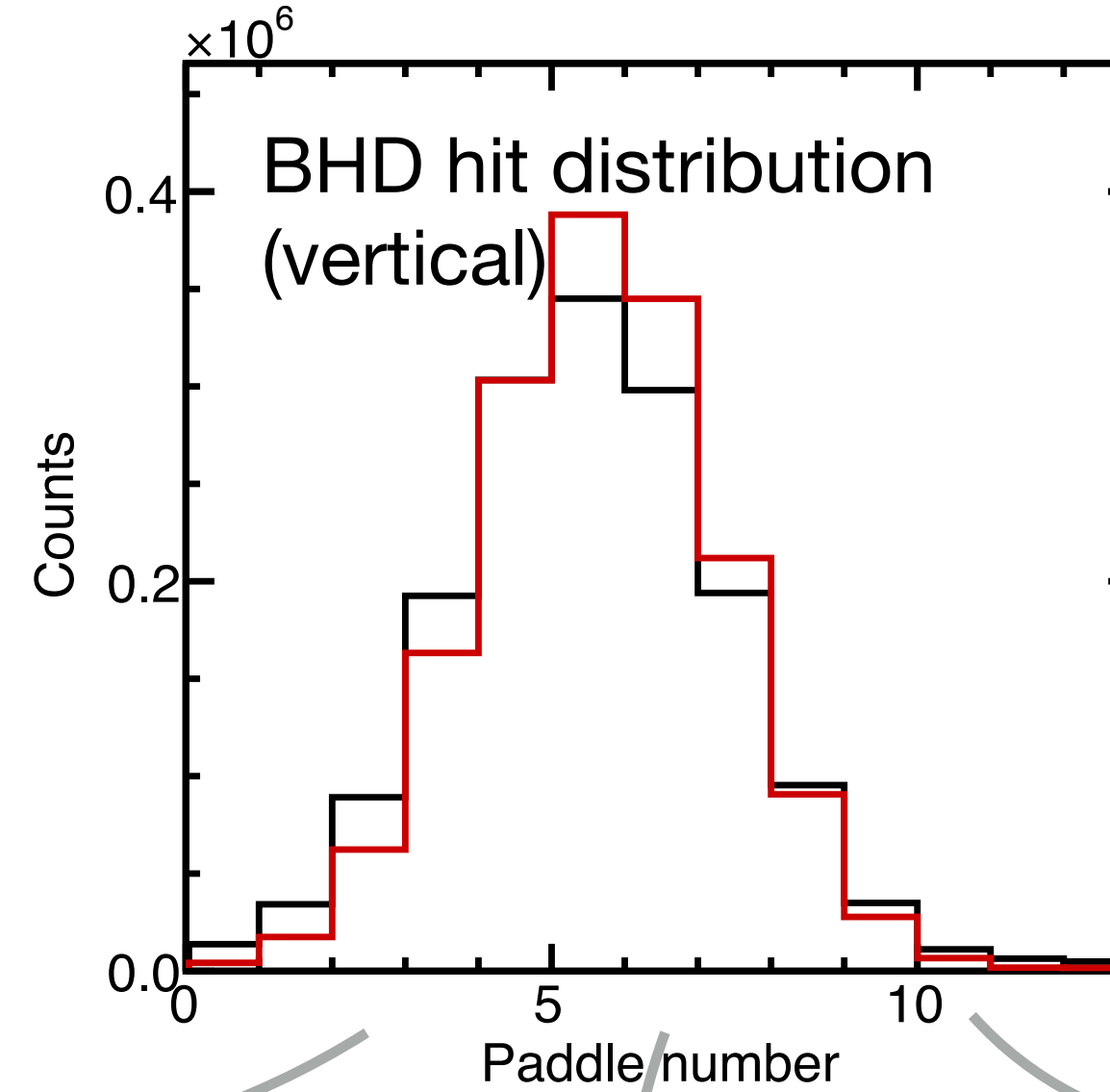
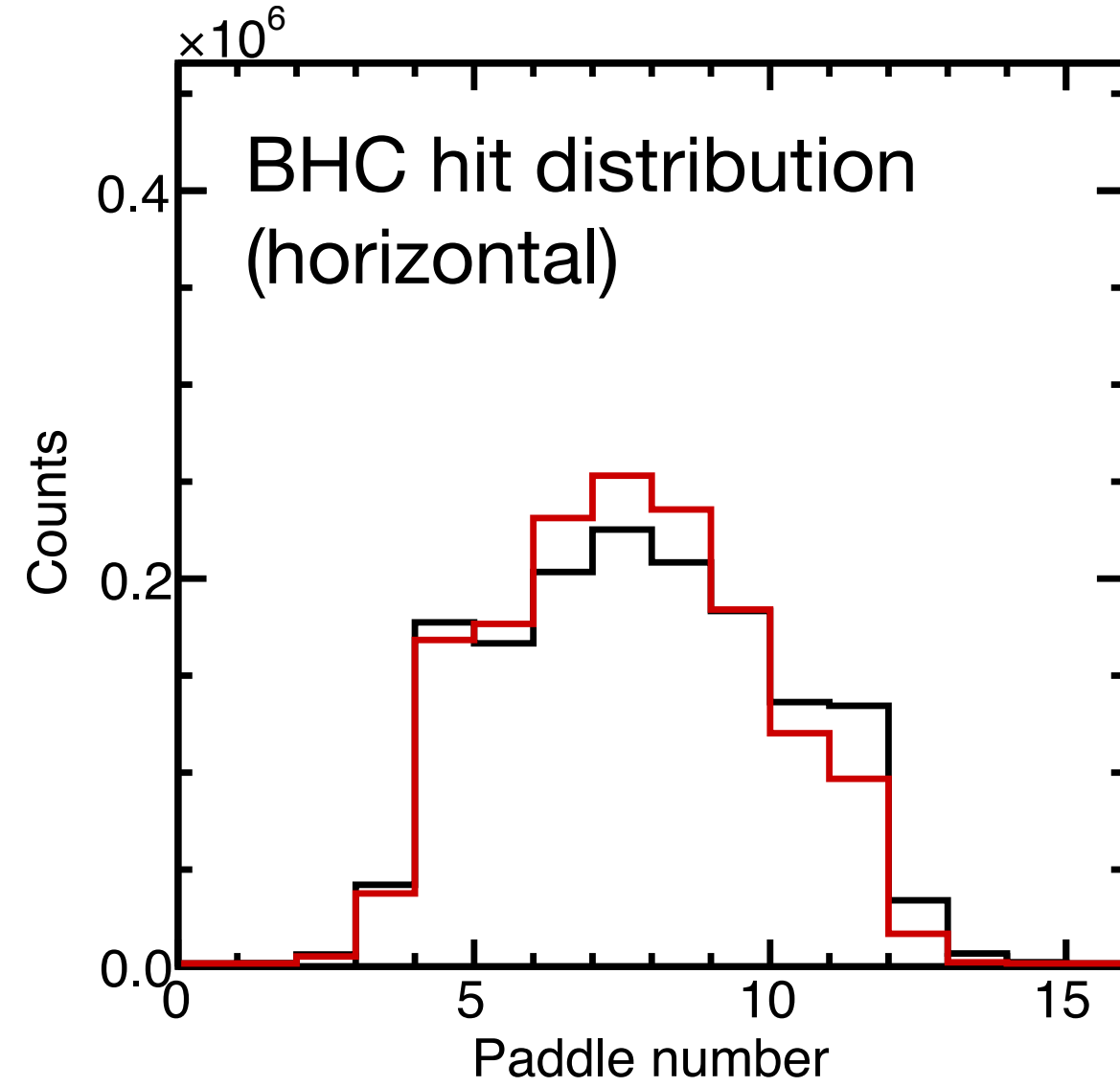
Effective speed of light: $c_{\text{eff}} \approx 14.5 \text{ cm / ns}$

Simulated light output and attenuation

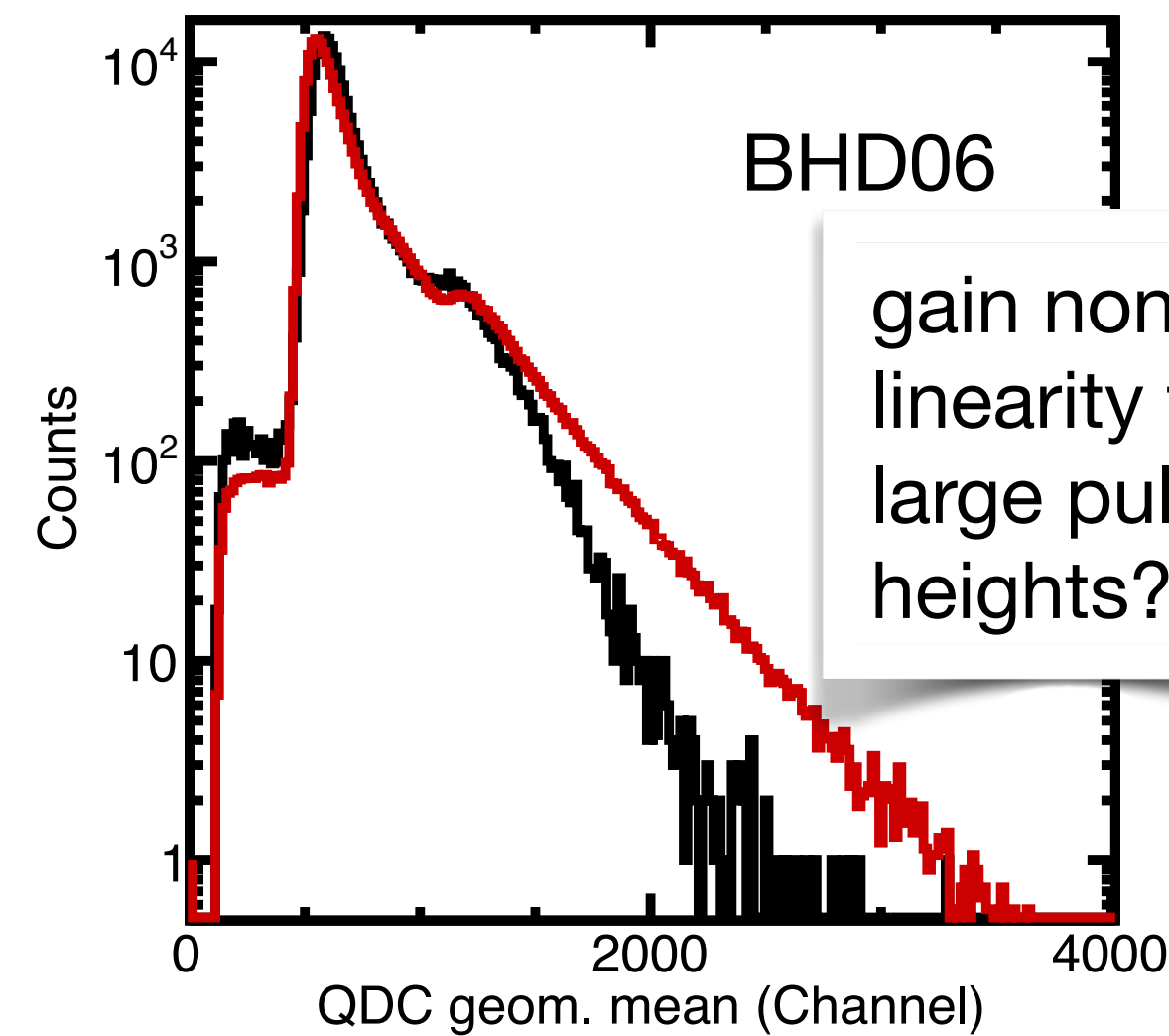
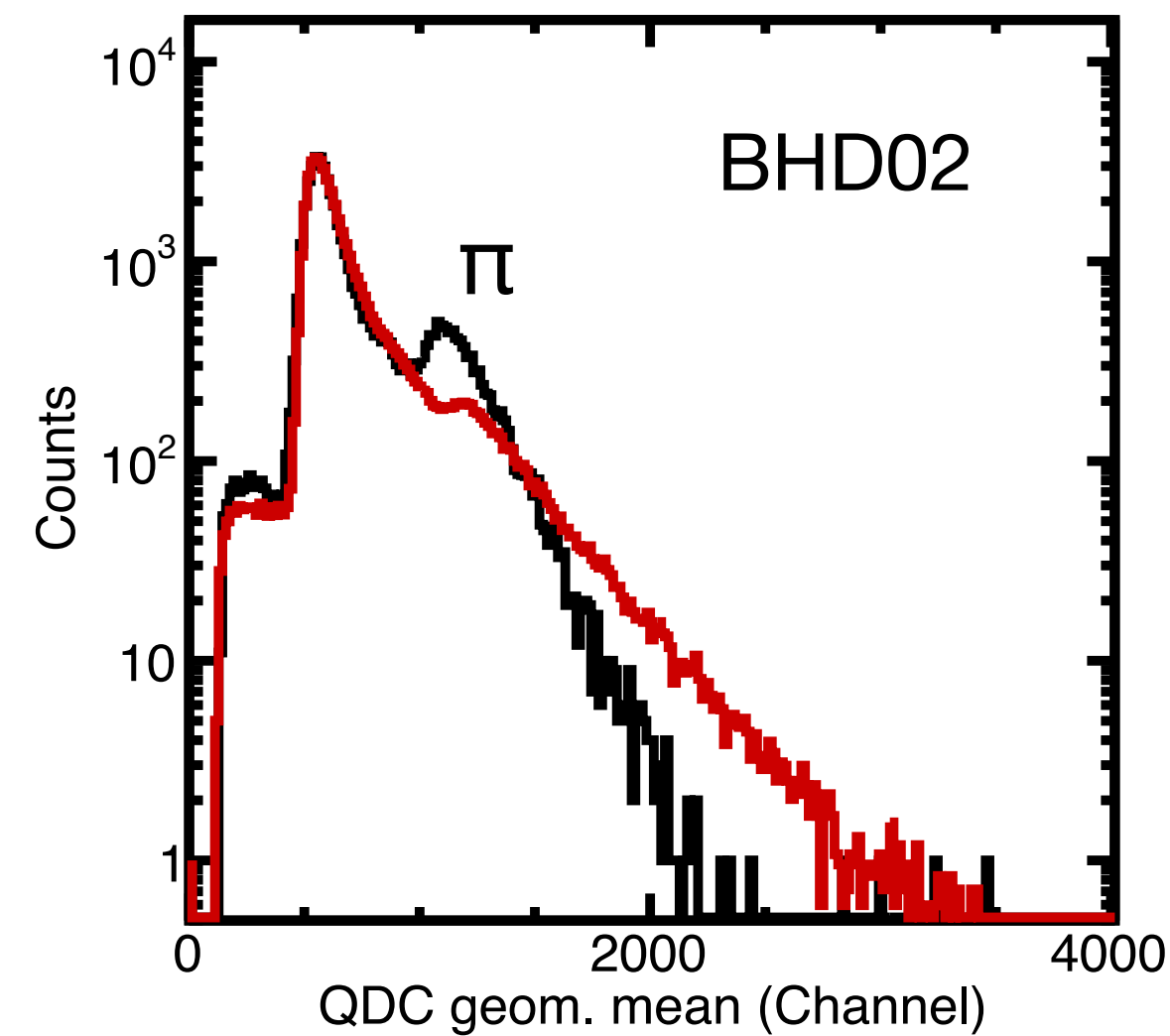


The pedestal to signal ratio and the below-threshold events are properly described by the simulation when the trigger on the SPSRF wall is considered.

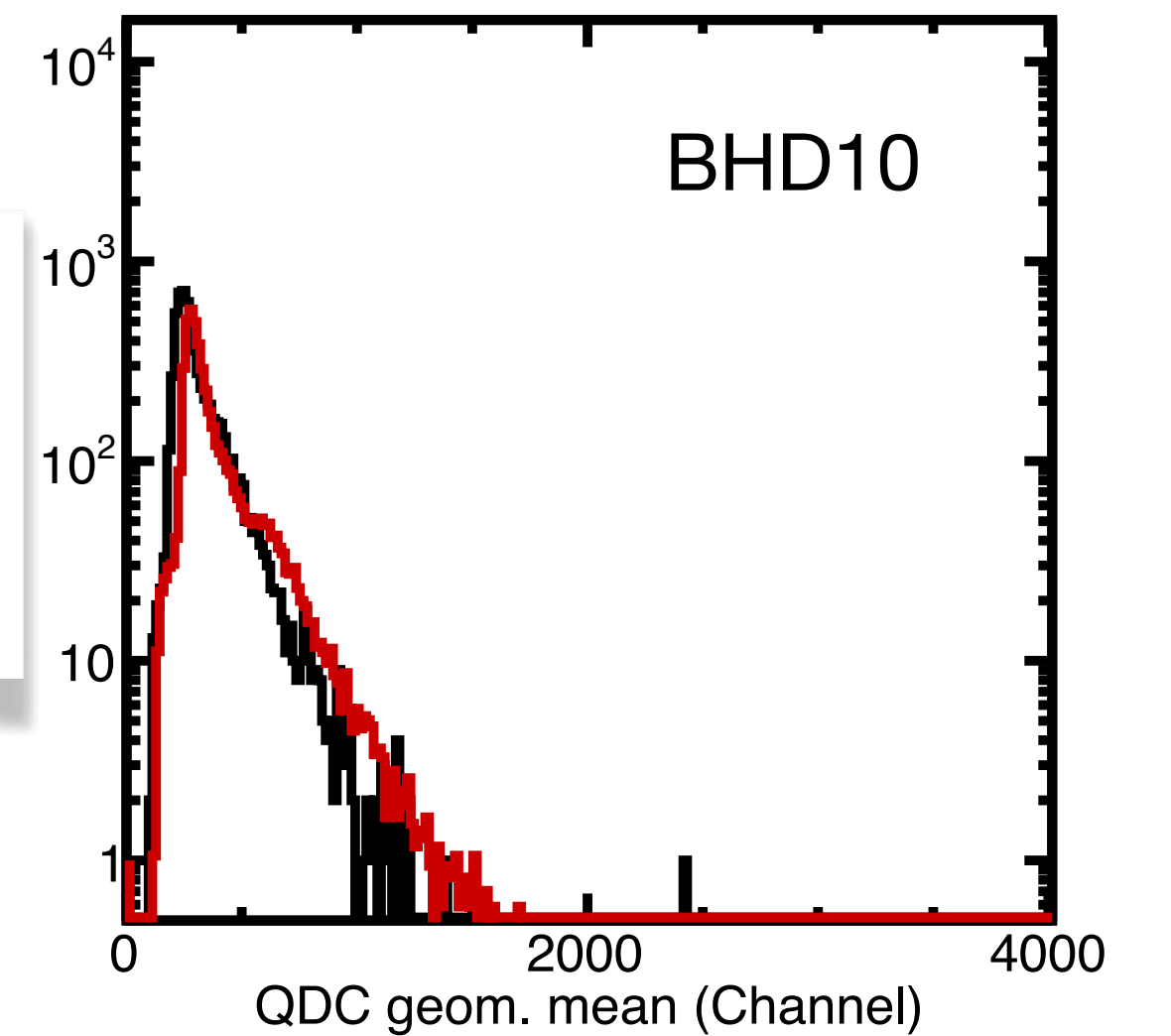
BH



— Data
— Simulation



gain non-linearity for large pulse heights?



relatively more pions in the data at the edge of the distribution

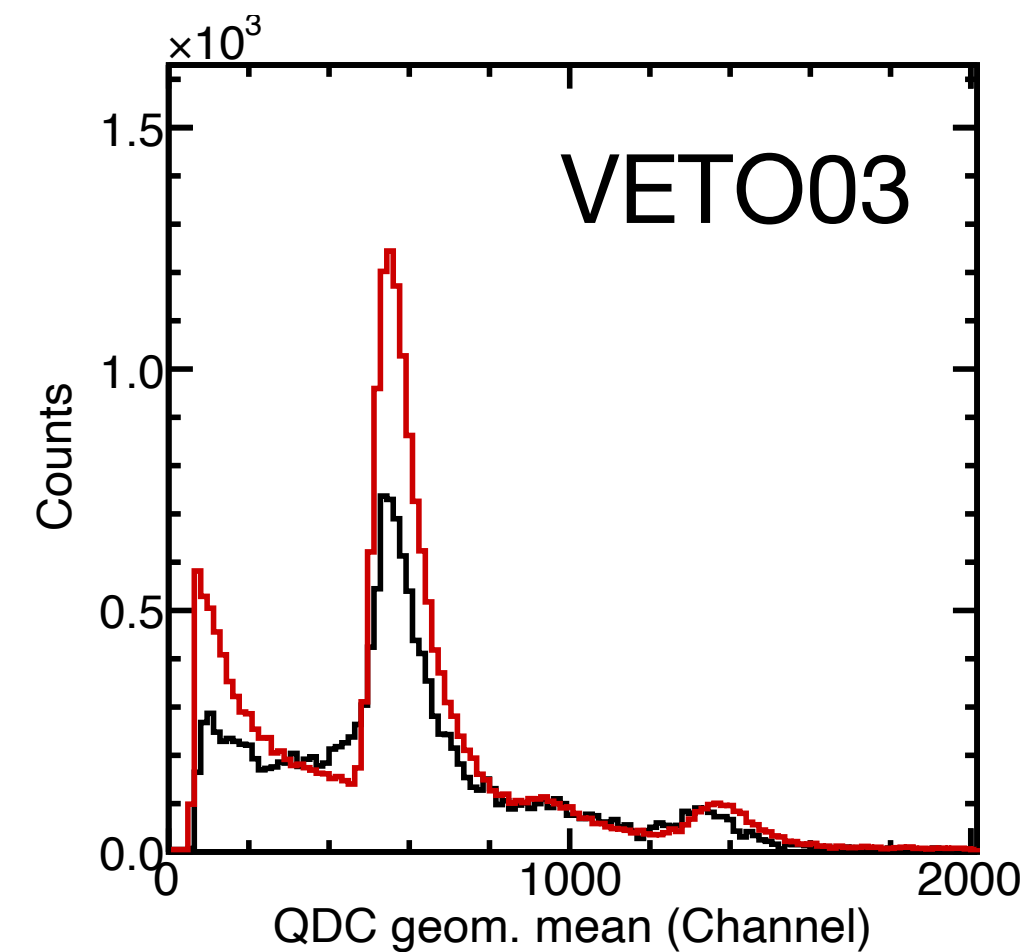
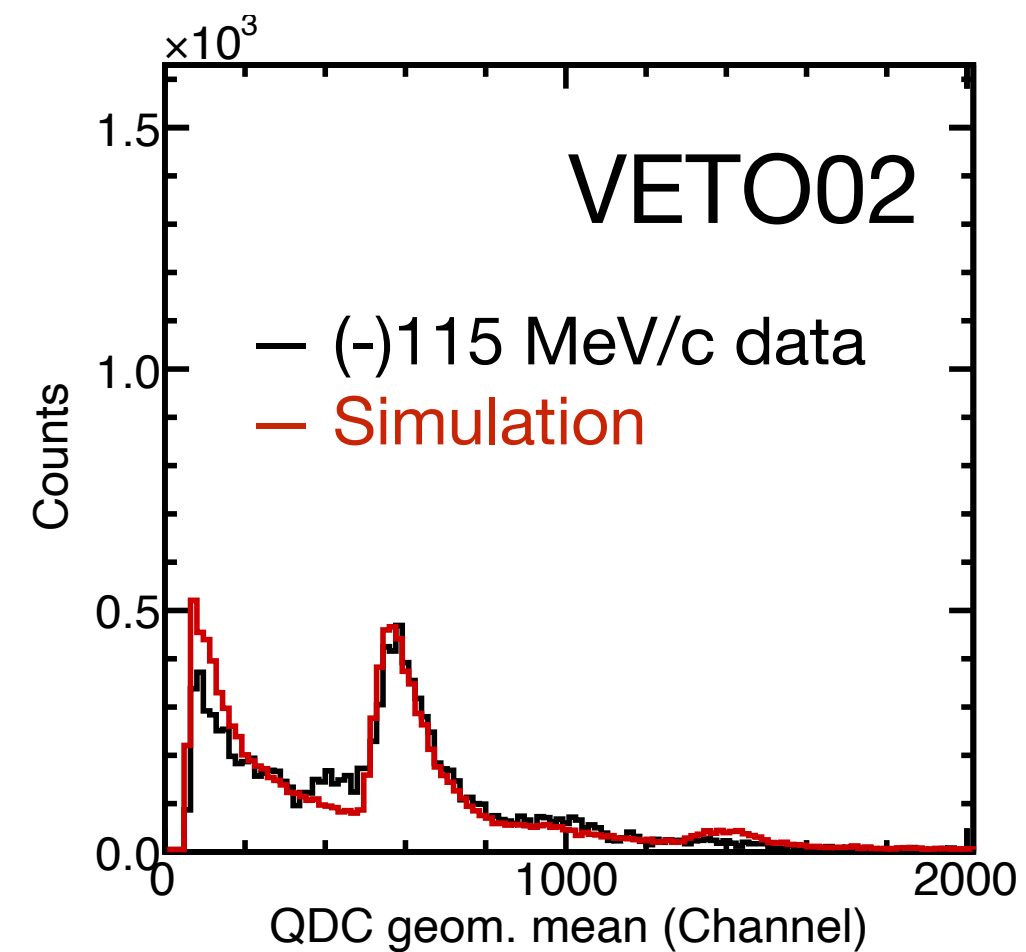
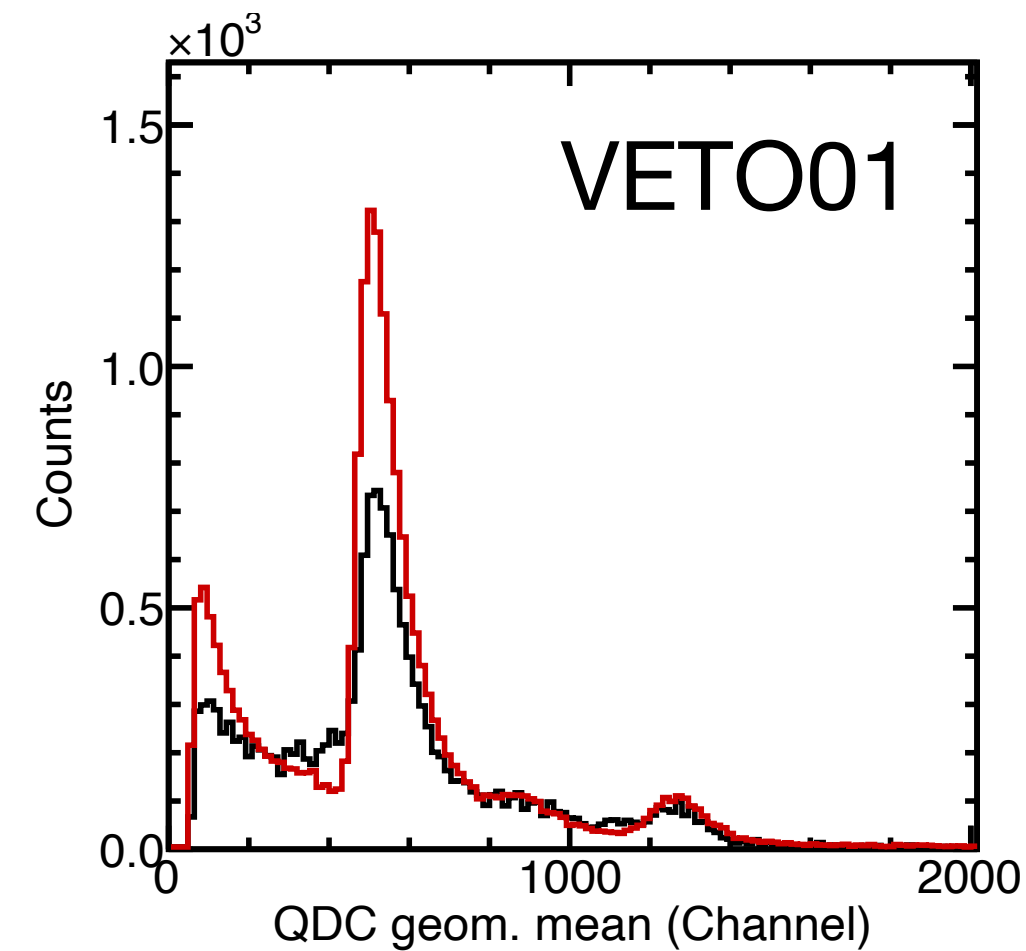
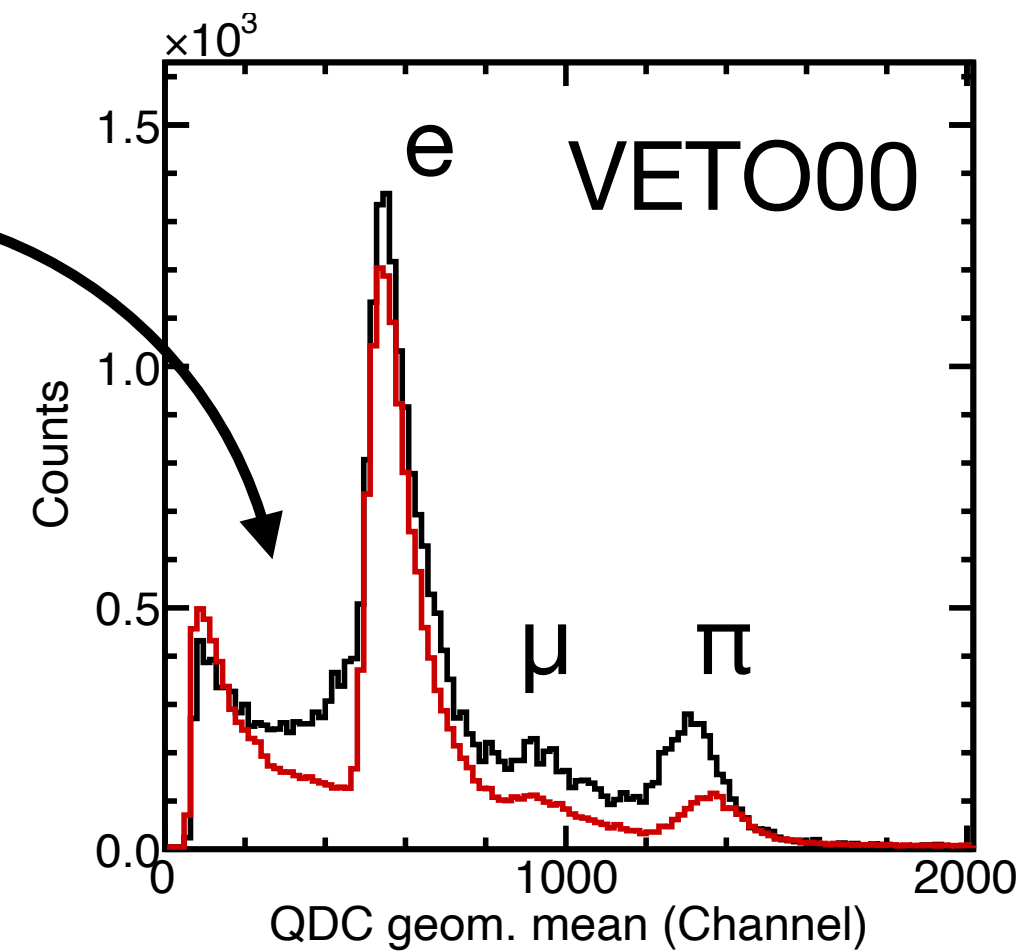
VETO

Larger variety of **energy depositions** in the experiment.

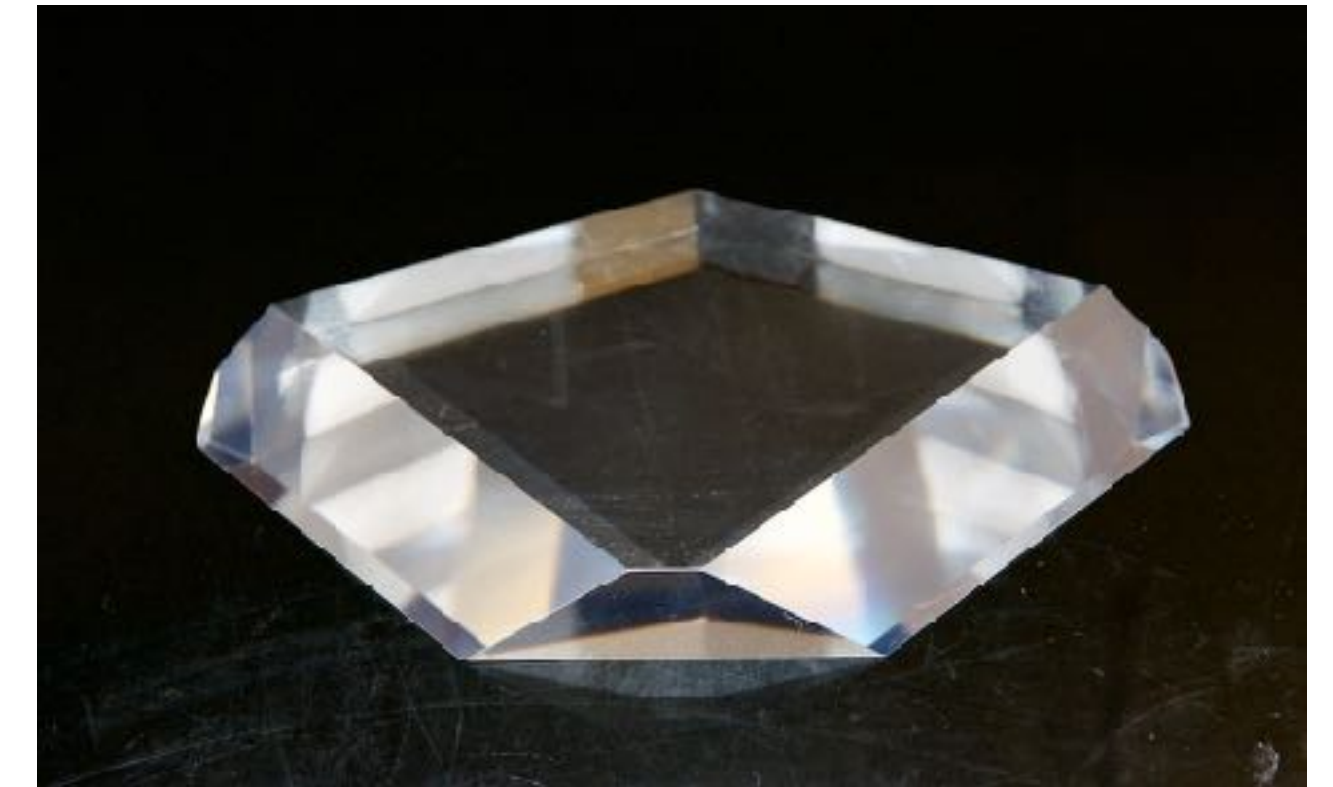
Yield fractions for various paddles are difficult to simulate:

- Beam tails
- Secondary particles

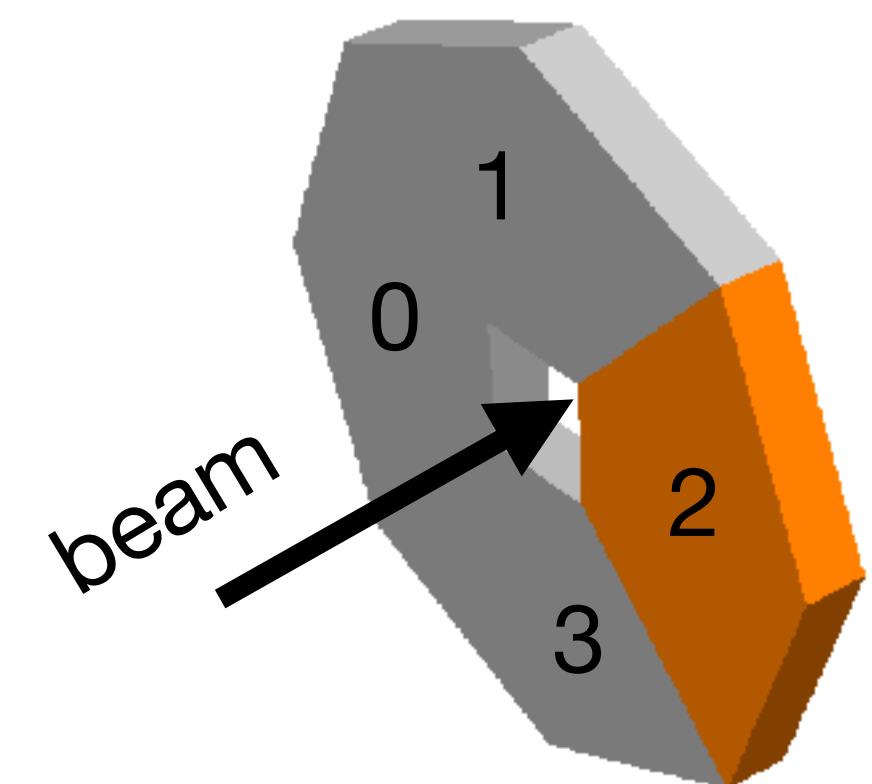
Particles hitting the VETO detector:
30% scattering-trigger events



VETO detector paddle

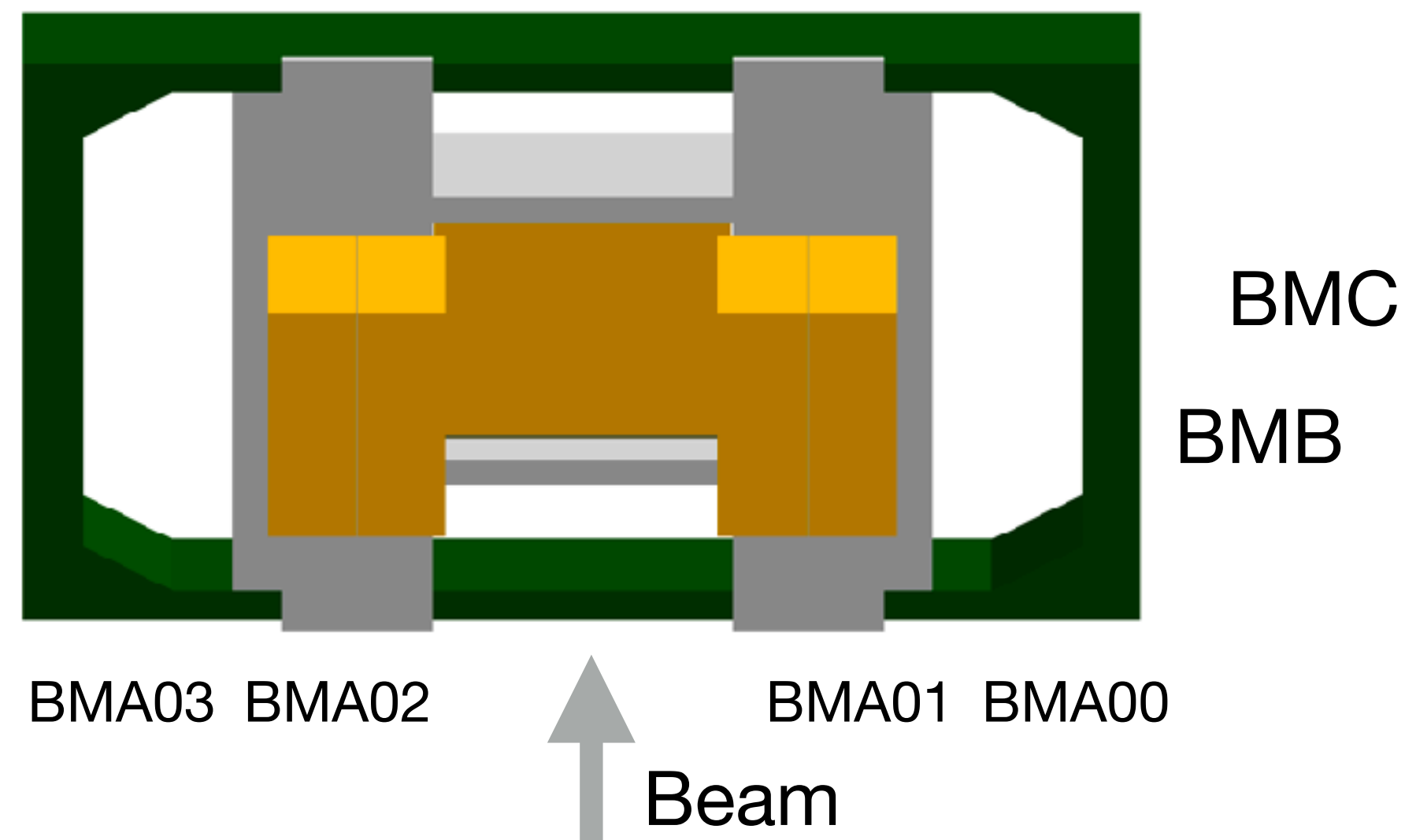
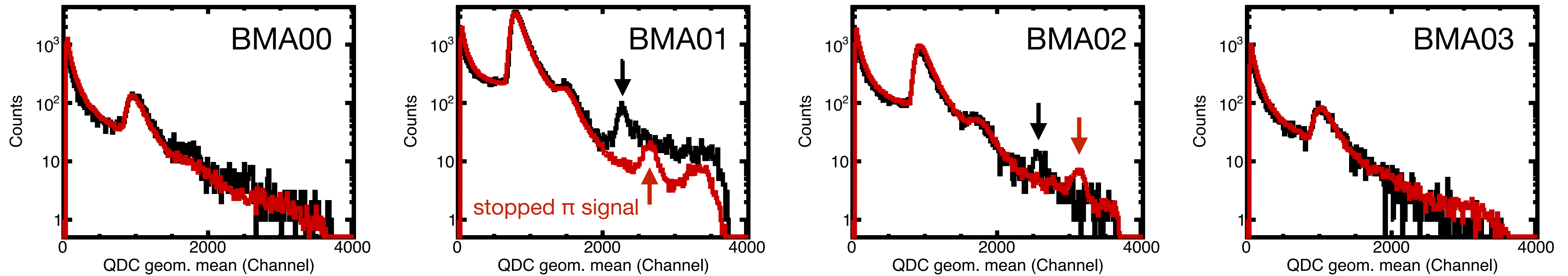


Simplified model of VETO detector paddle in the simulation.



BM – Energy deposition

— (-)115 MeV/c data
 — Simulation



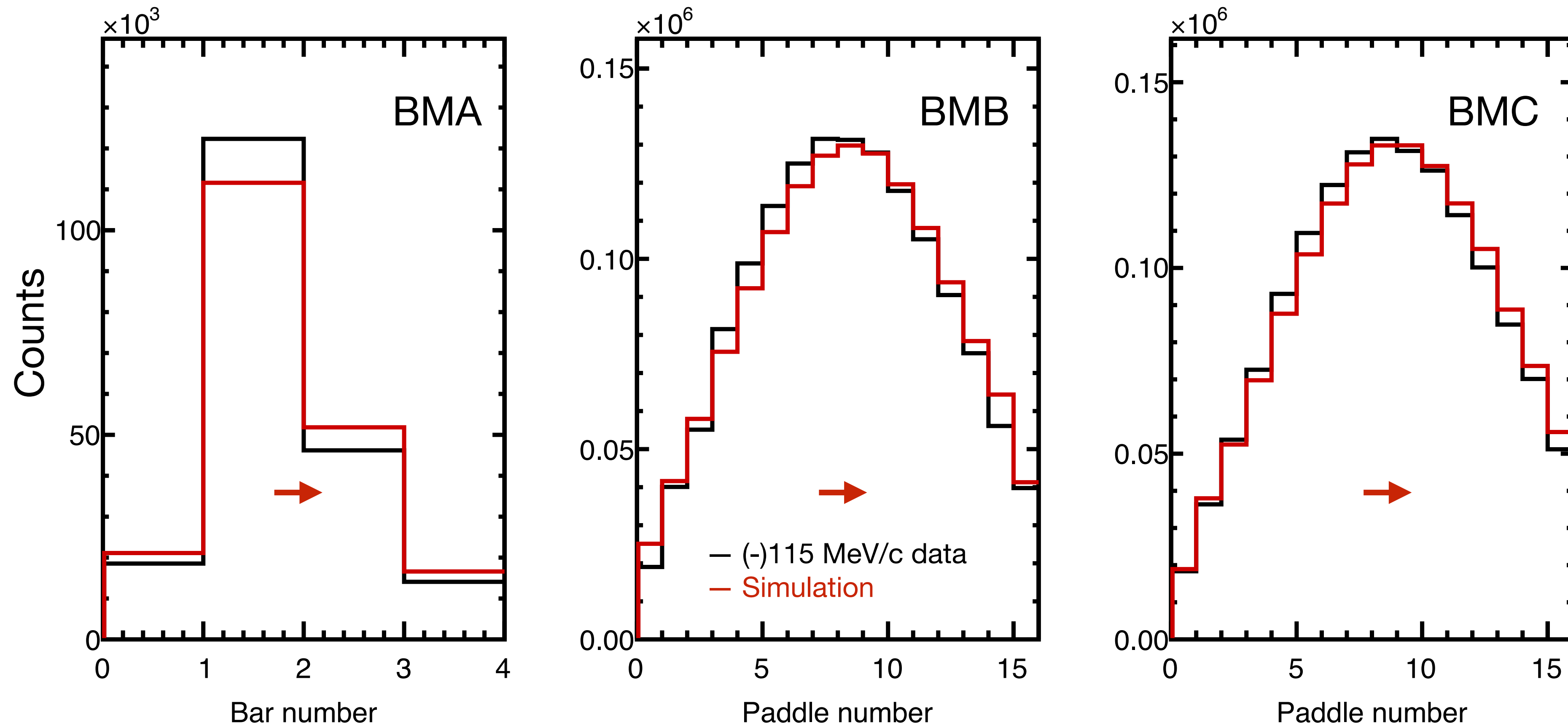
π stopped in the inner two BMA bars, but no evidence of pions reaching outer two BMA bars.

Excellent agreement for electron and muon energy depositions.

Mismatch of measured and simulated stopped- π energy deposition:

- gain non-linearity, saturation?
- too narrow integration gate?
- energy degradation of π not in the simulation?

BM — Hit distributions well described



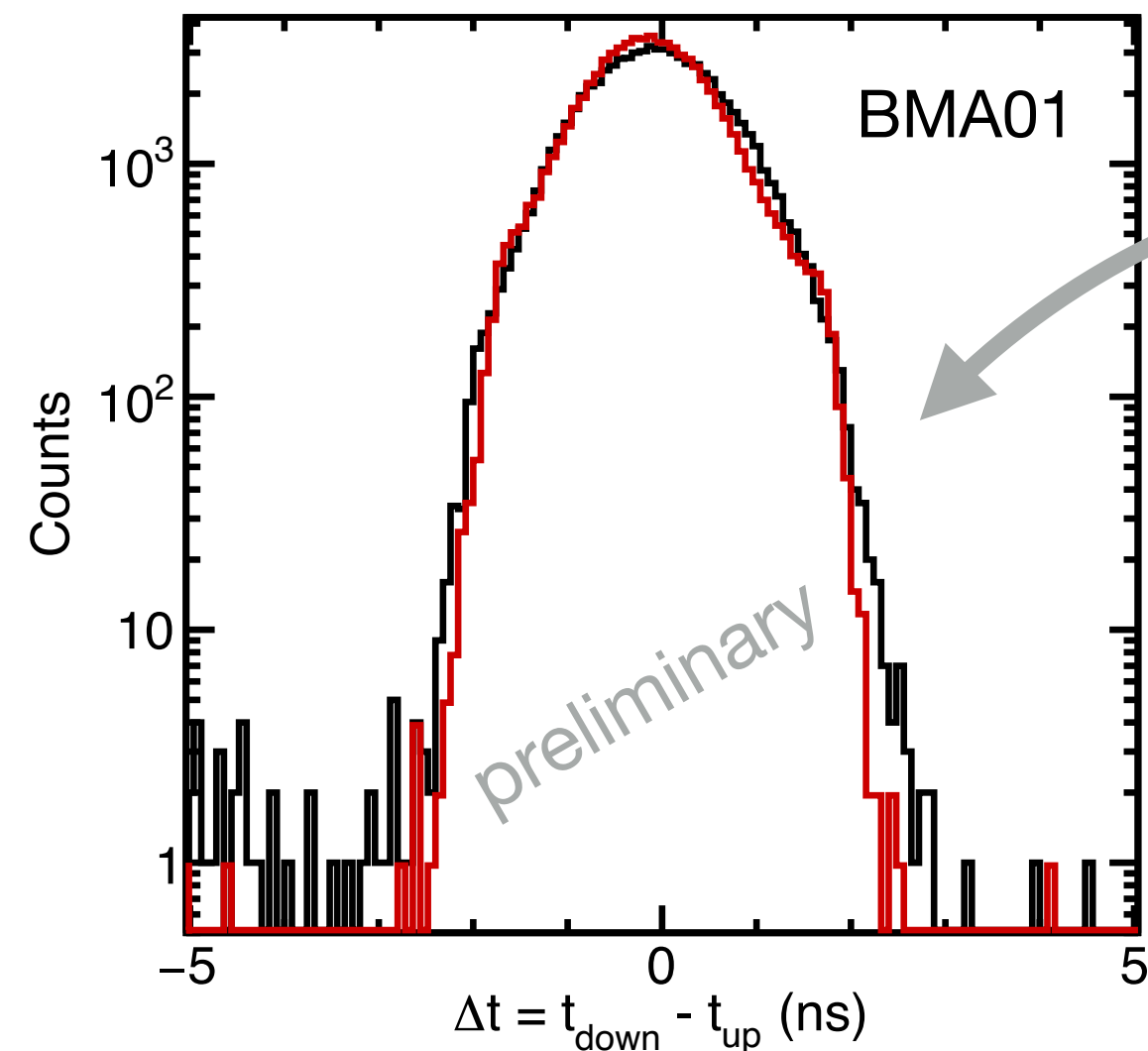
Tool to constrain beam parameterization for the simulation?

Simulated beam possibly shifted by 1/3 of a paddle width to larger paddle numbers (beam left), this corresponds to 2 mrad as seen from GEM0.

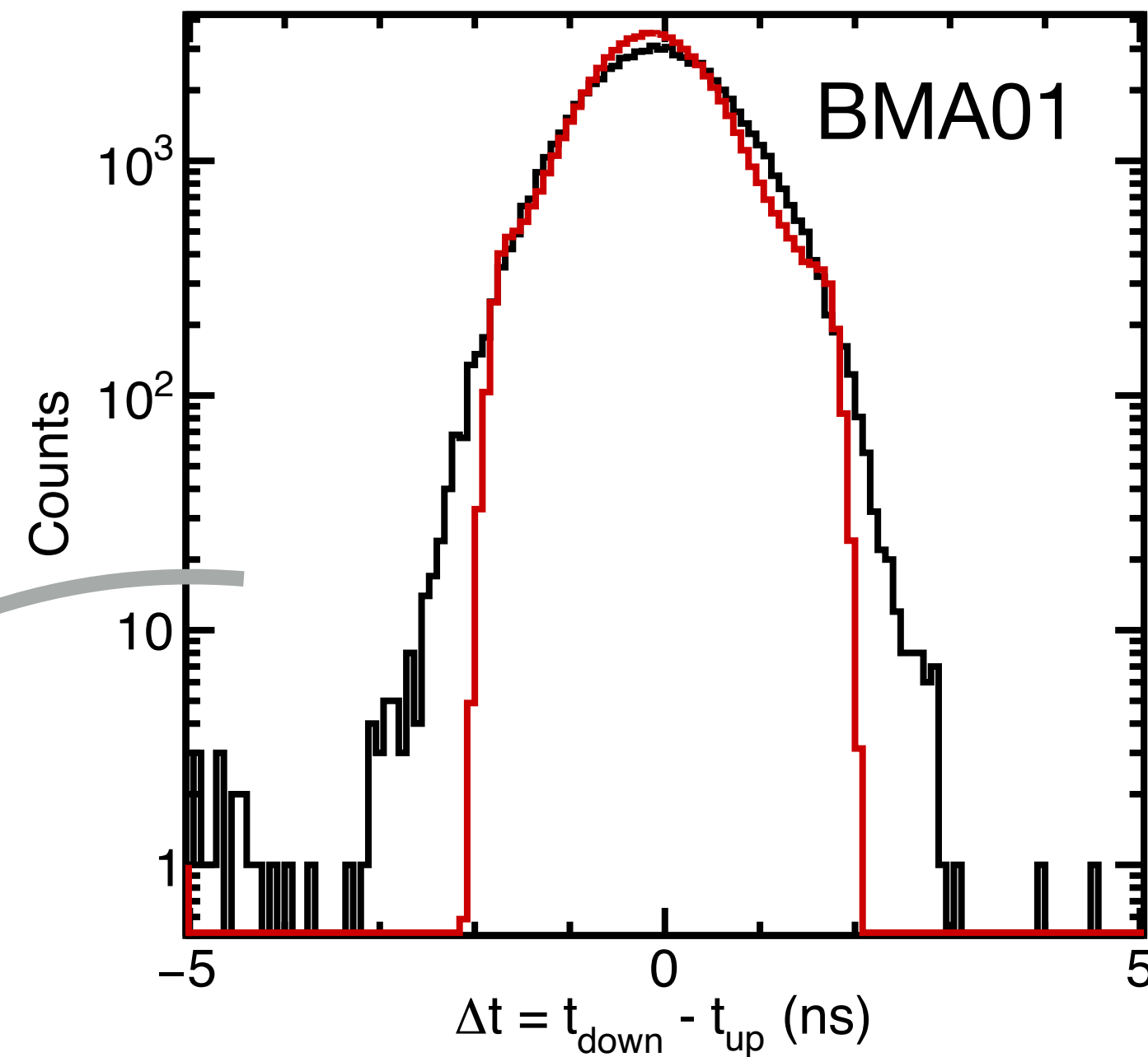
BM time resolution

BM read uses constant-fraction discriminators

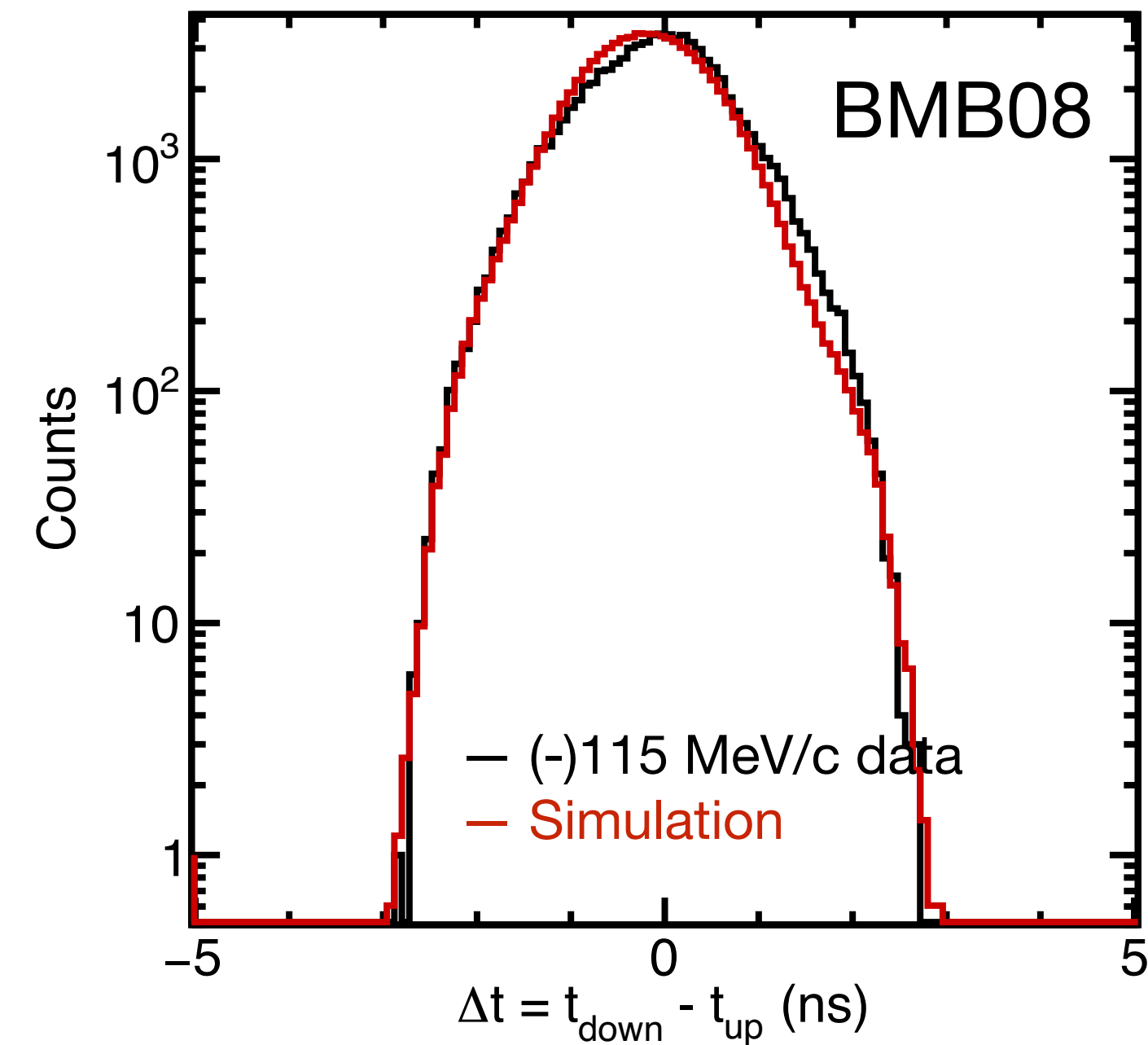
Nevertheless, the time-resolution can be improved with additional time-walk corrections



BMA: fair description with the assumed time resolution of $\sigma(t_{\text{mean}}) = 35 \text{ ps}$



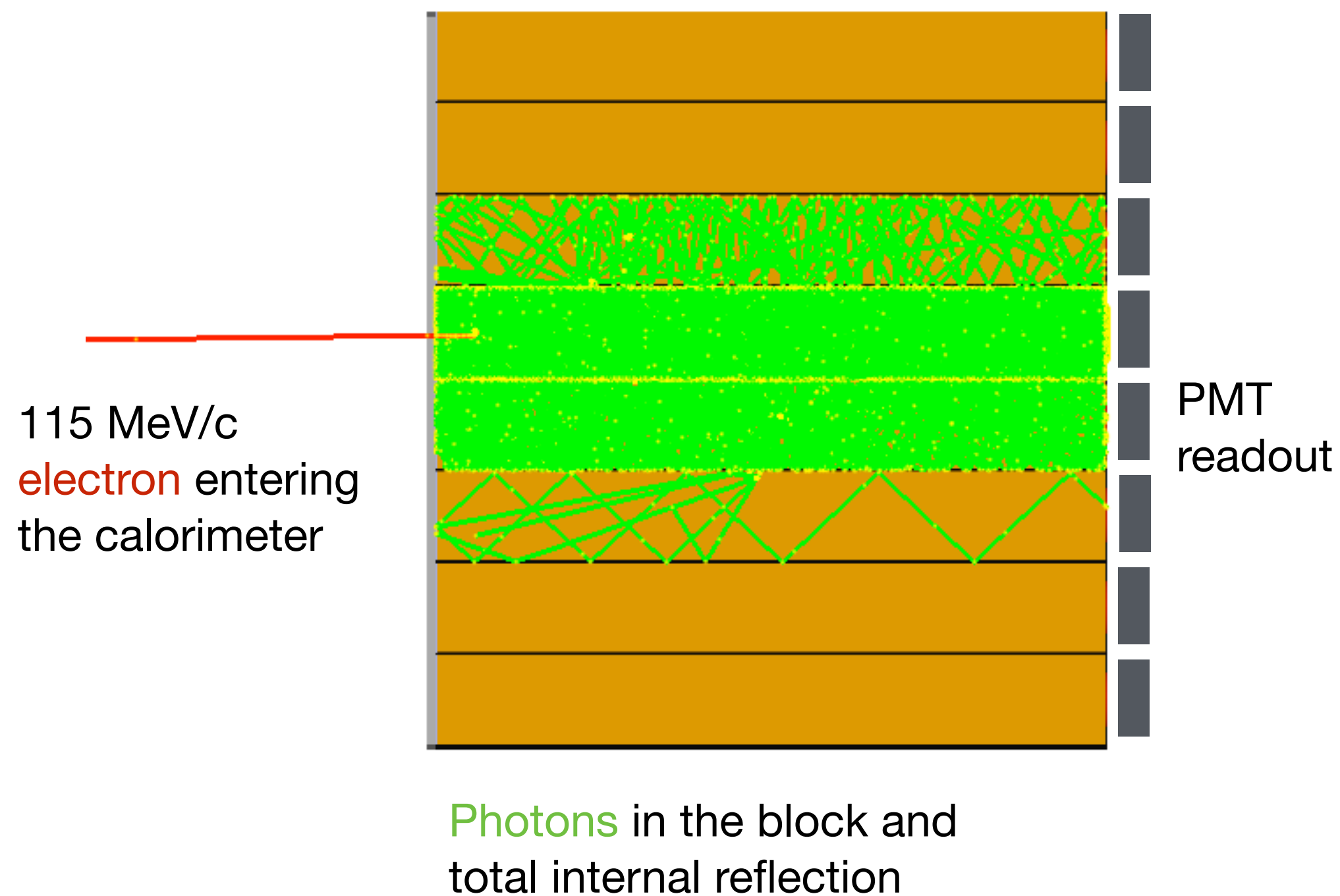
BMB, BMC: good description with the assumed time resolution of $\sigma(t_{\text{mean}}) = 100 \text{ ps}$



Expected width of the Δt distribution for 30-cm long scintillators: $\pm 2 \text{ ns}$

Simulation and digitization of lead-glass Cherenkov detector

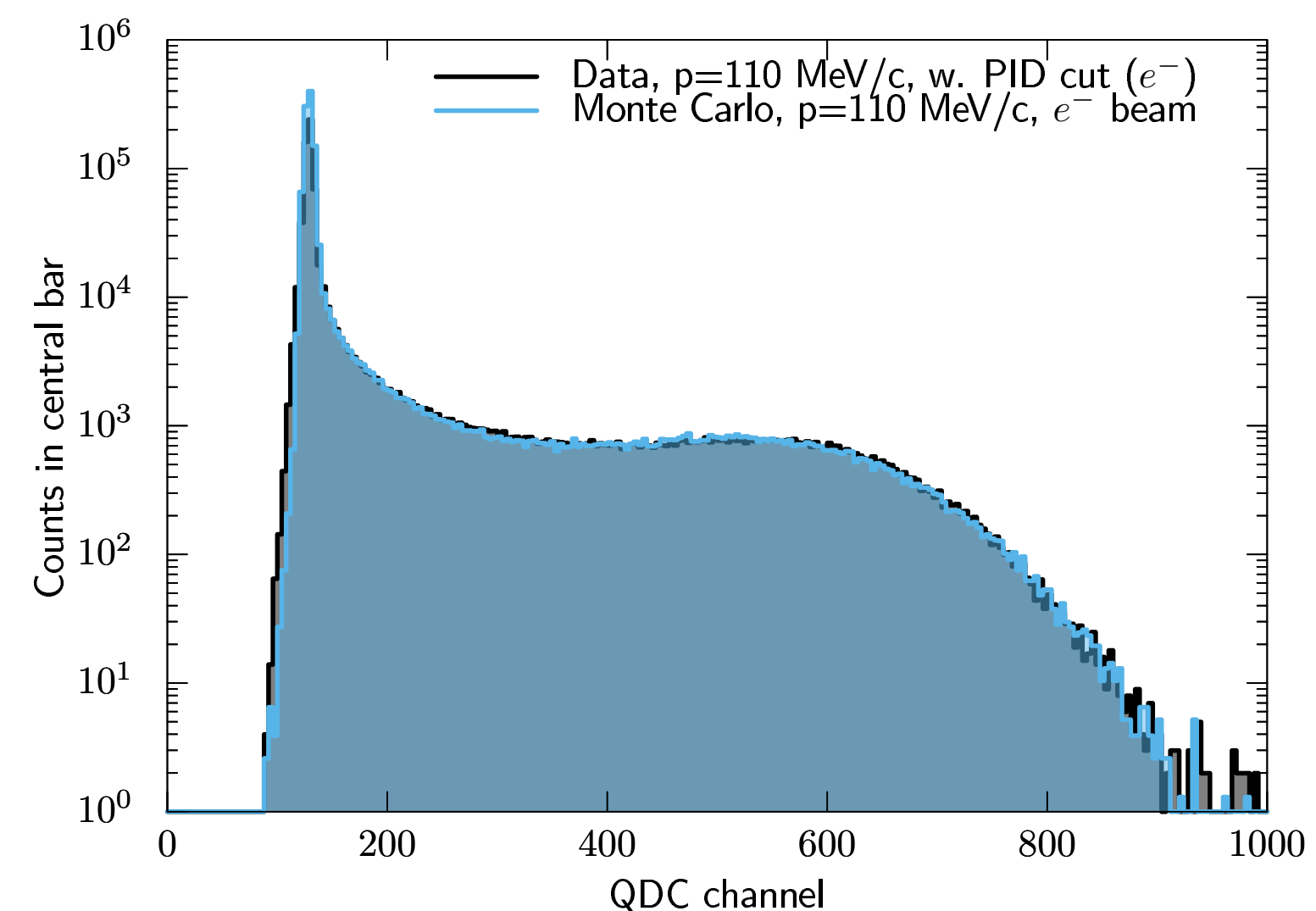
Method A: Cherenkov light production and photon transport by Geant4. Accumulate photon yield, Y , at the site of the PMT.



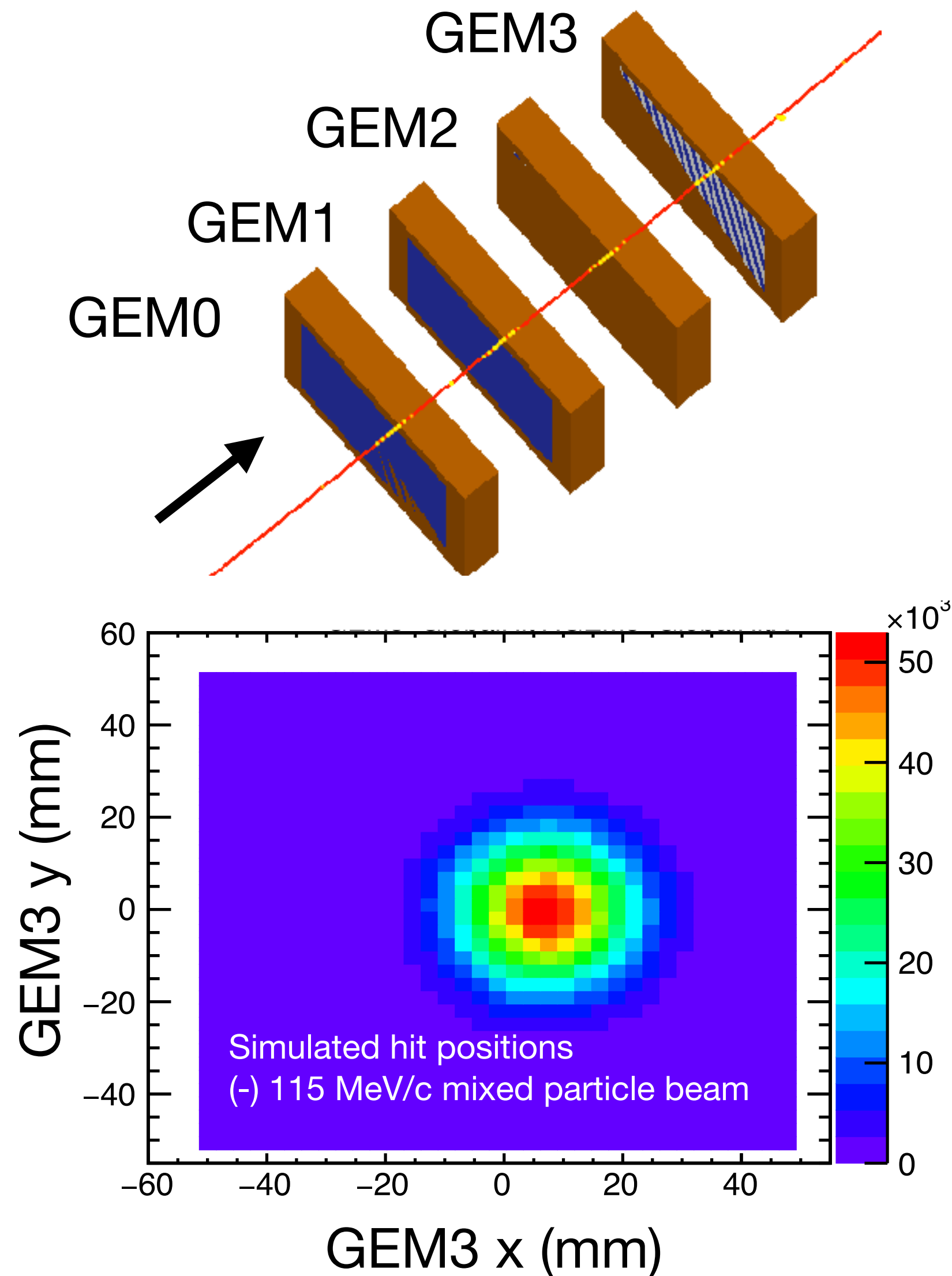
Method B (fast): Estimate the number of Cherenkov photons from the speed of the particle:

$$Y \propto \int 1 - \frac{1}{n^2\beta(x)^2}$$

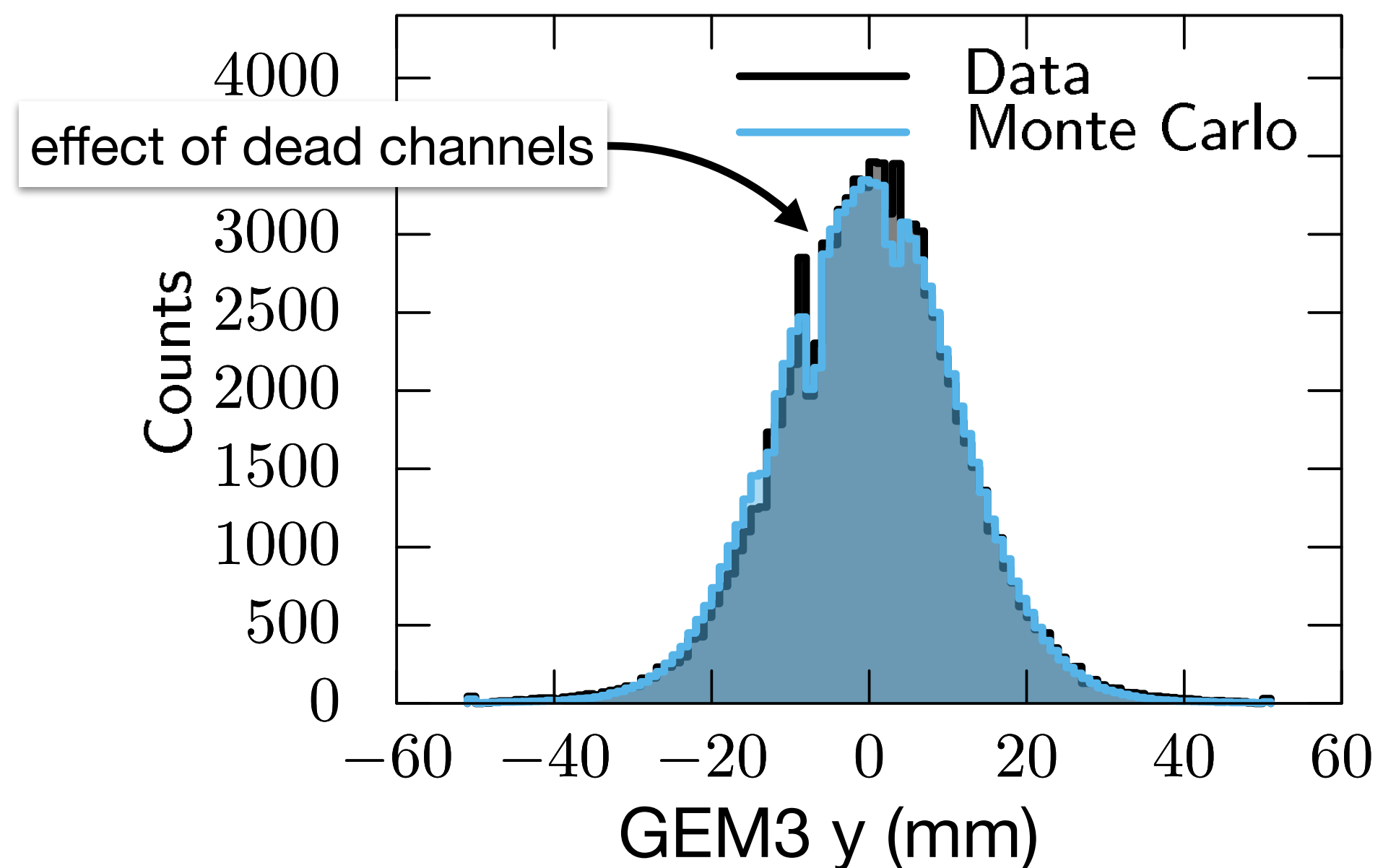
Digitization: Conversion of light-output Y to QDC values (pedestal, gain per lead-glass element, resolution).



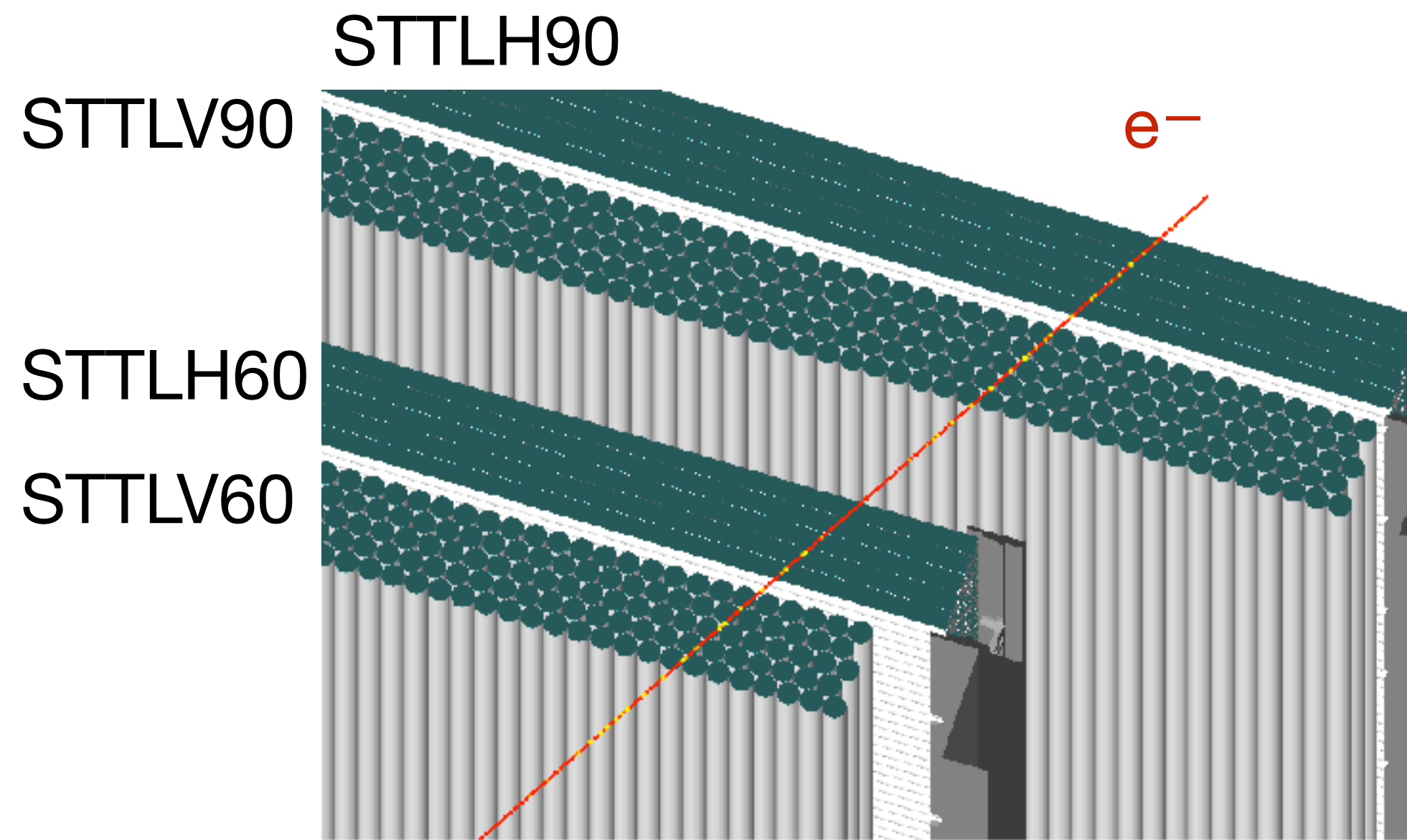
GEM digitization of simulated data



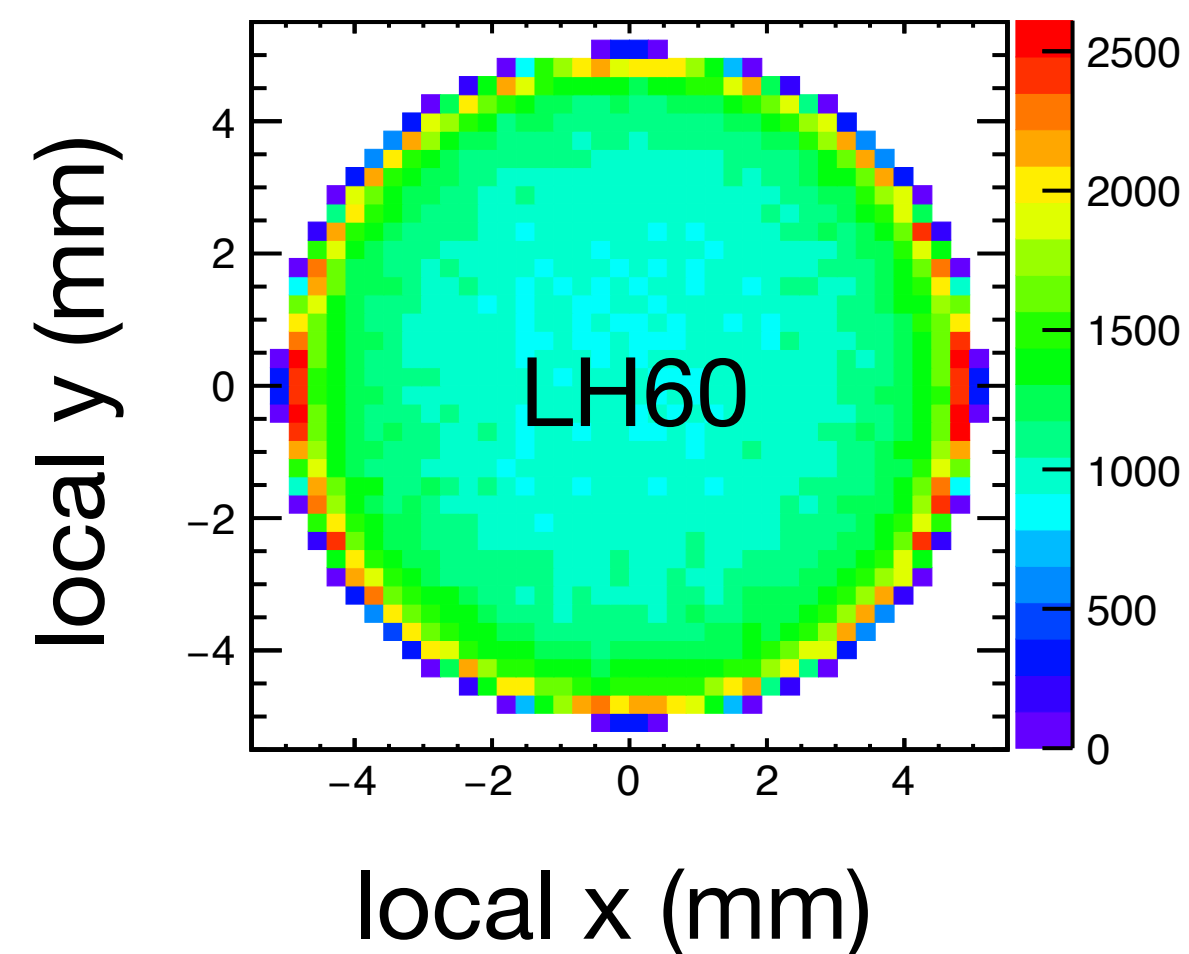
- Mapping of hit position into struck strip numbers for both axis
- Modeling of hit pattern on strips
- Suppression of dead channels
- Conversion to ADC values (including channel pedestal, and with currently fixed gain, noise)
- Per APV common mode noise



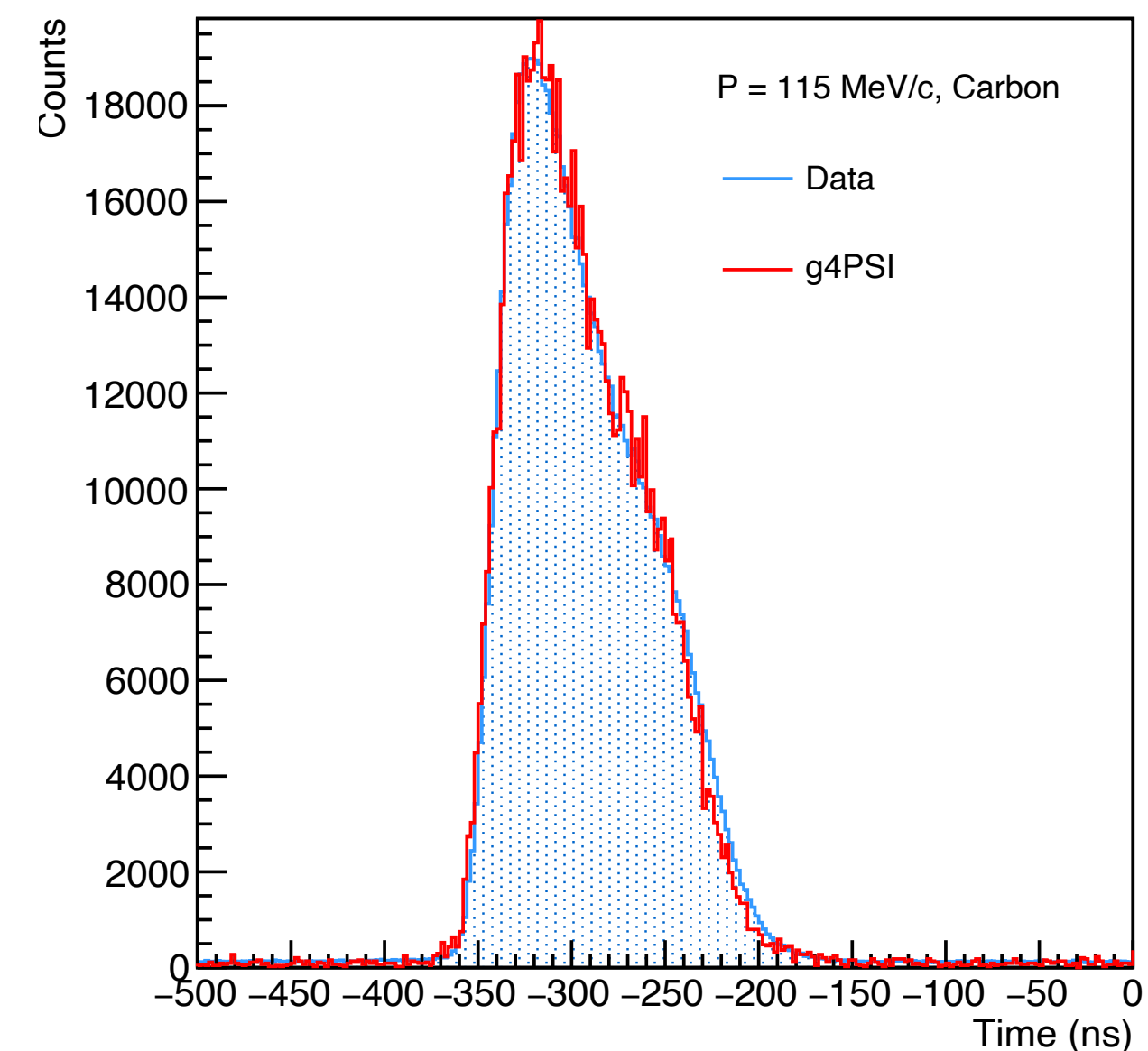
STT digitization of simulated data



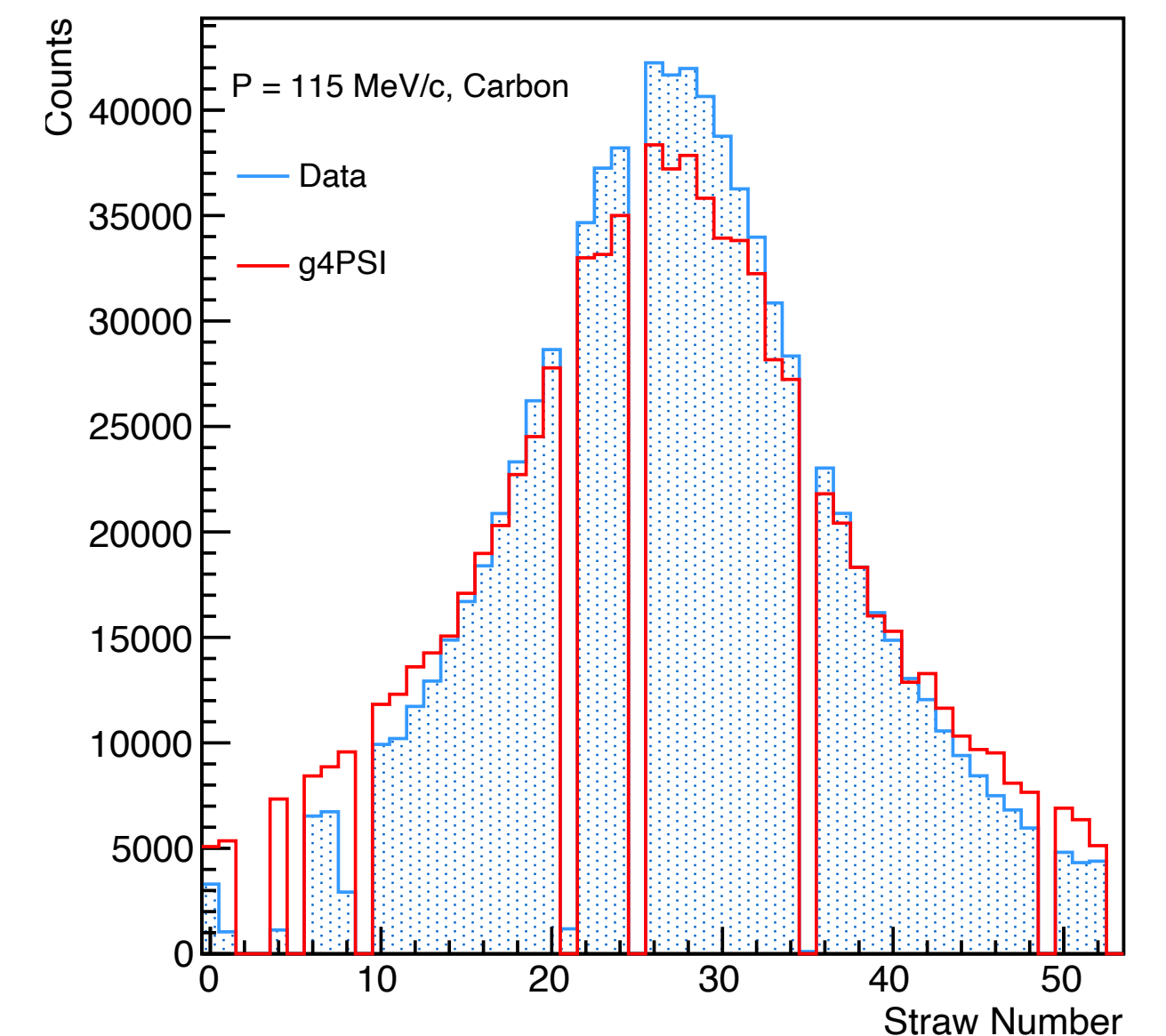
- Straws are identified by copy-ID numbers
- Local hit positions and directions are converted to drift distances and drift times that include effective resolutions
- Suppression of dead channels



Drift-time distribution
LH60 Plane 1



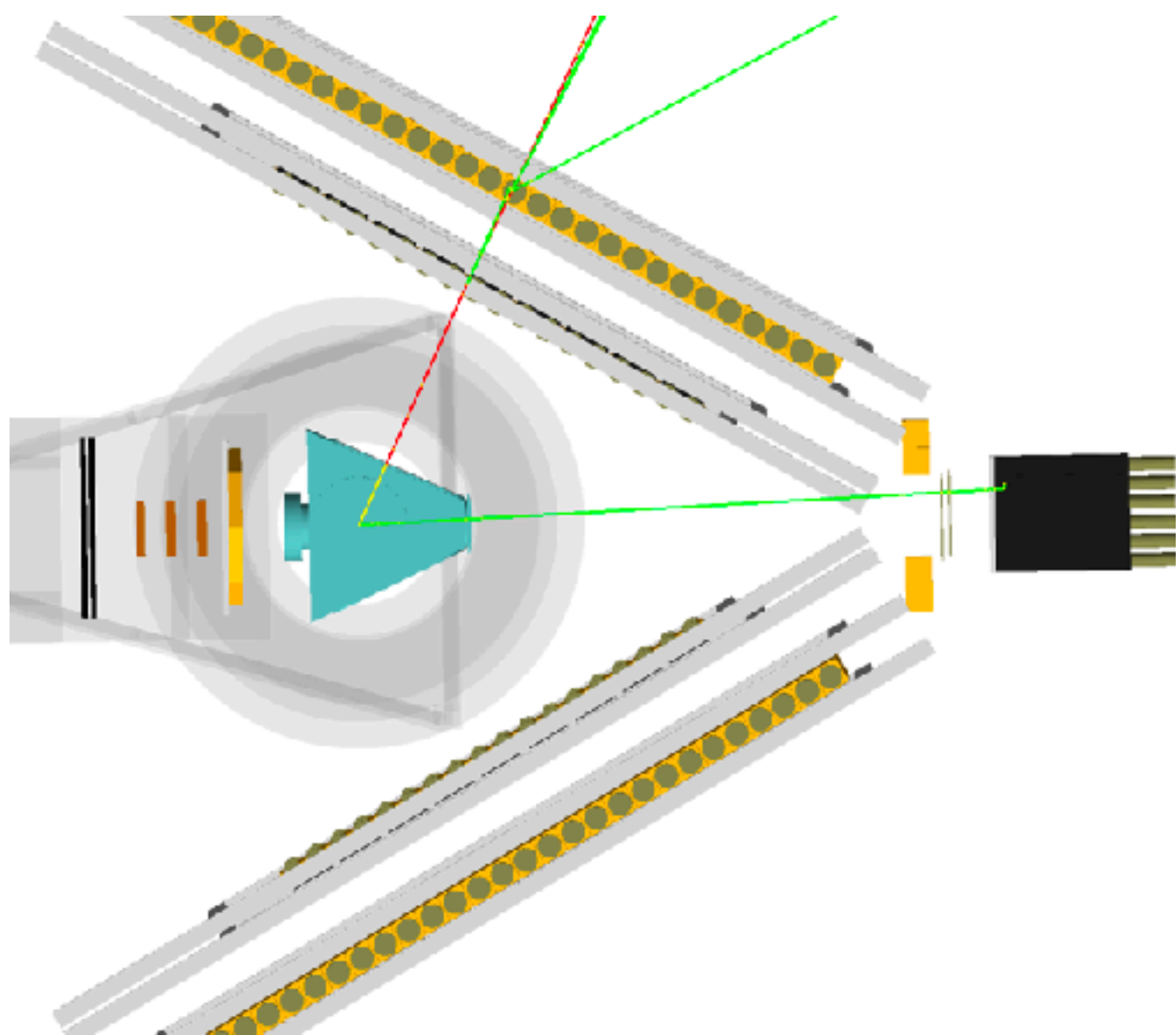
Straw distribution
LH60 Plane 1



ESEPP in g4PSI - initial version

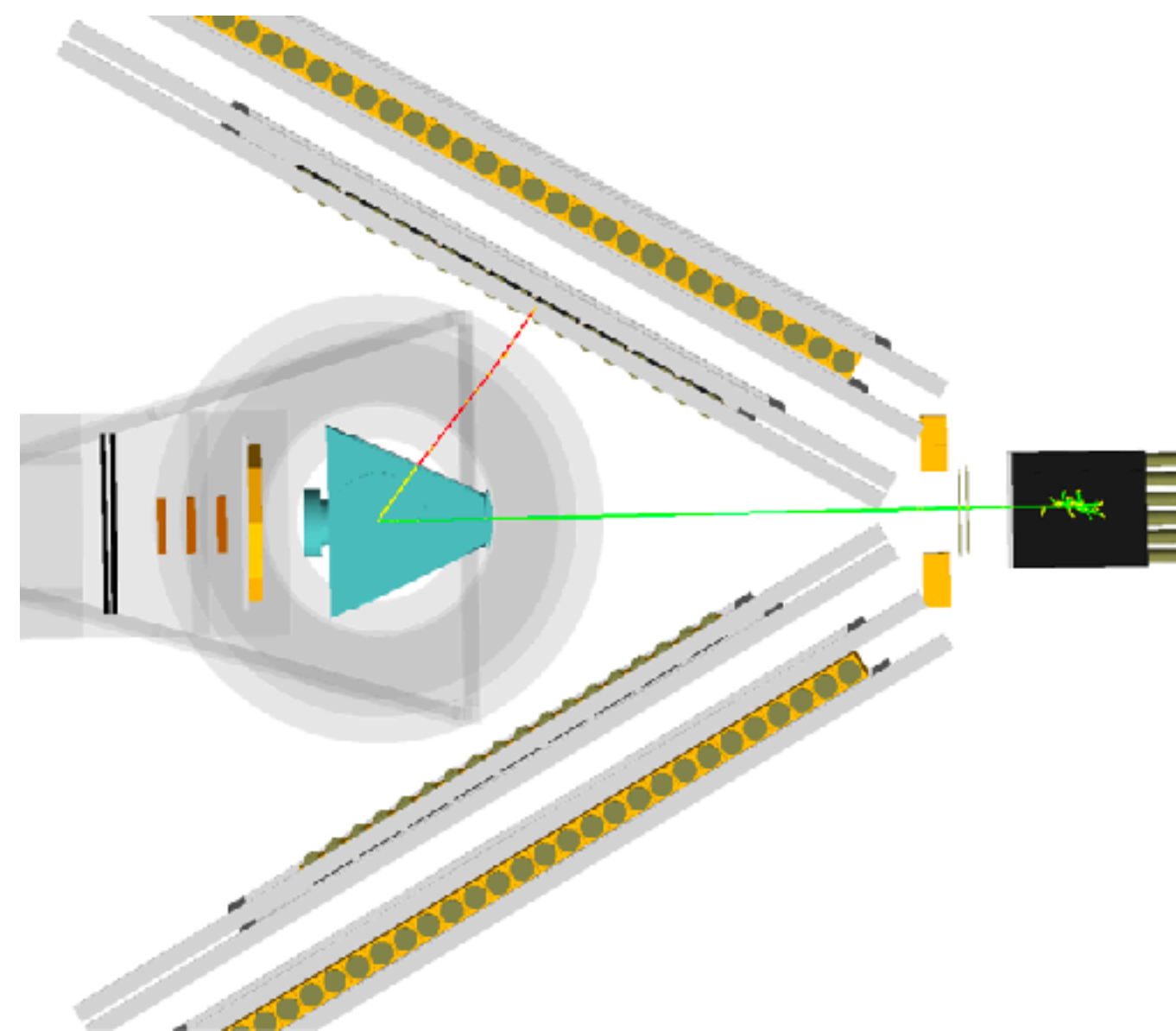
Examples: $ep \rightarrow e'p\gamma$

$$p_0 = 161 \text{ MeV/c}$$
$$\theta \approx 60^\circ$$



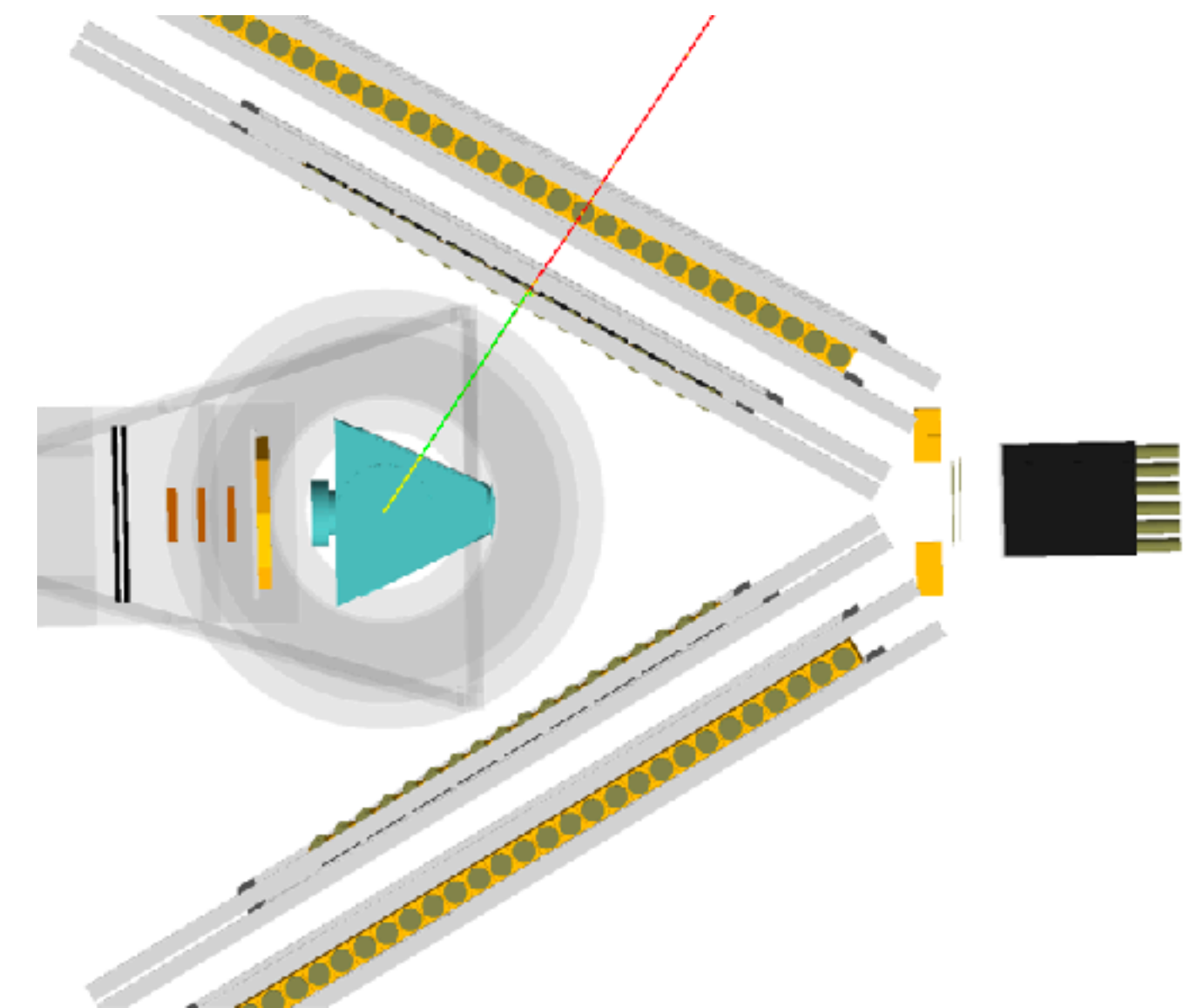
Initial-state radiation
low photon energy

$$p'_e > p'_{min}$$



Initial-state radiation
high photon energy

$$p'_e < p'_{min}$$



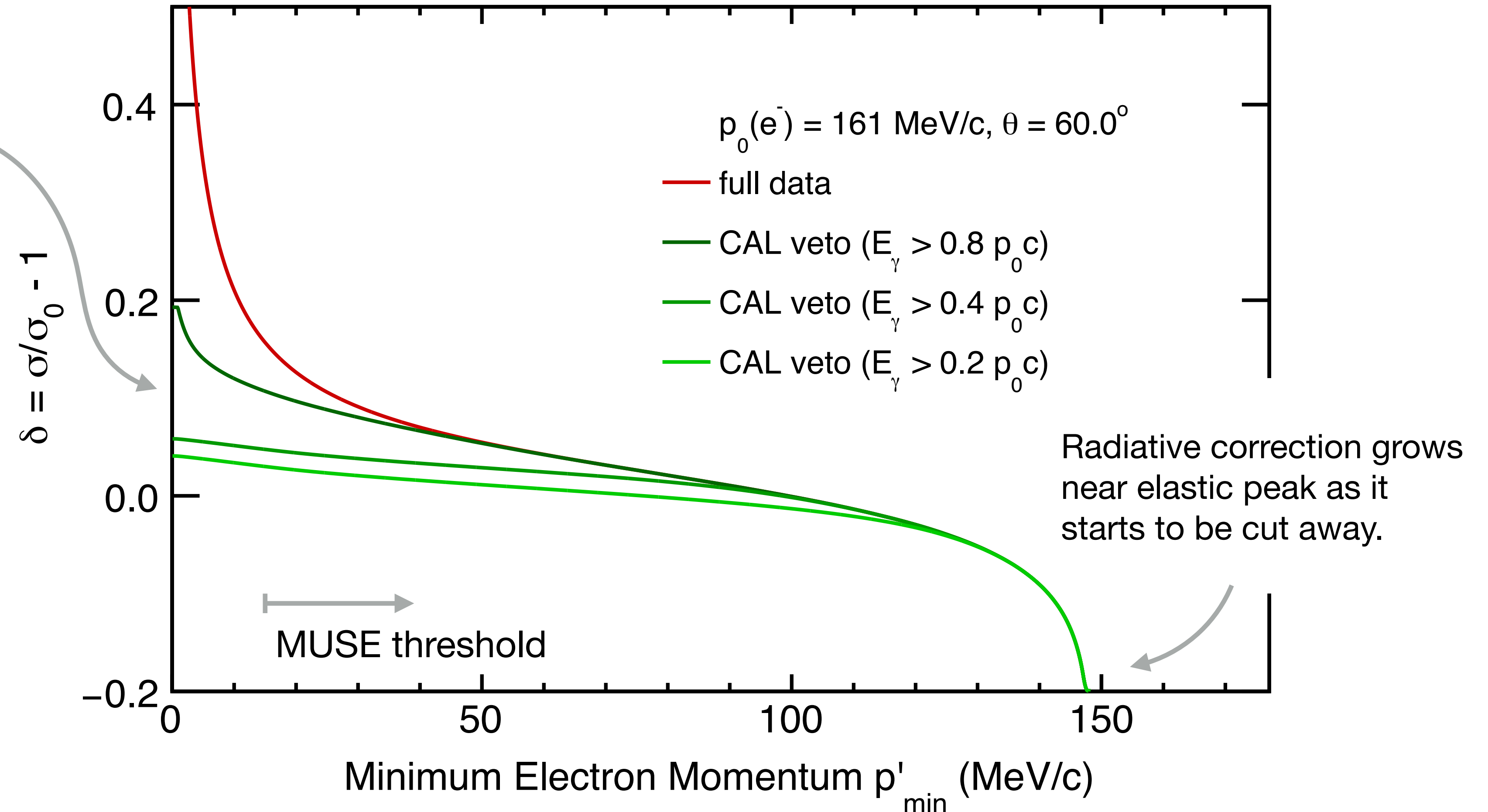
Final-state radiation

Radiative corrections for e^-p scattering data in MUSE kinematics

CAL veto on downstream photons reduces radiative corrections and p'_{\min} dependence, reducing uncertainty.

The preliminary estimates of the total uncertainties in the radiative corrections for electrons are **0.2% - 0.5%**.

Angle-dependent uncertainty, relevant for radius extraction, \approx **0.3%**.



Much more work to be done ...

- Geometry
 - Include all relevant structure material (in/out scattering, background source)
 - Setup and alignment (run-time dependent)
- Running the simulation
 - Finalize model and tune of particle beams
 - Rare-event Simulations
 - Include relevant physics processes (radiative processes)
- Digitization
 - Finalize the implementation of the digitization methods
 - Digitization of trigger conditions, as well as RF and trigger times
 - Tune of detector parameters (run-time dependent)
 - Slow-control data in the simulation output